Title

Salmonella multimutants enable efficient identification of SPI-2 effector protein function in gut inflammation and systemic colonization

Authors

Joshua P. M. Newson[1], Flavia Gürtler[1,2], Pietro Piffaretti[1], Annina Meyer[1,3], Anna Sintsova[1], Manja Barthel[1], Yves Steiger[1], Sarah C. McHugh[1,4], Ursina Enz[1], Neal M. Alto[5], Shinichi Sunagawa[1], Wolf-Dietrich Hardt[1]

Affiliations

1. Institute of Microbiology, ETH Zurich, Zurich, Switzerland
2. Current address: Epidemiology, Biostatistics & Prevention Institute, University of Zurich, Zurich, Switzerland
3. Current address: Institute of Food, Nutrition and Health, ETH Zurich, Zurich, Switzerland
4. Current address: Department of Fundamental Microbiology, University of Lausanne, Lausanne, Switzerland
5. Department of Microbiology, University of Texas (UT) Southwestern Medical Center, Dallas, TX, United States.

Correspondence

hardt@micro.biol.ethz.ch

newsonj@ethz.ch

Abstract

Salmonella enterica spp. rely on translocation of effector proteins through the SPI-2 encoded type III secretion system (T3SS) to achieve pathogenesis. More than 30 effectors contribute to manipulation of host cells through diverse mechanisms, but interdependency or redundancy between effectors complicates the discovery of effector phenotypes using single mutant strains. Here, we engineer six mutant strains to be deficient in cohorts of SPI-2 effector proteins, as defined by their reported function. Using various animal models of infection, we show that three principle phenotypes define the functional contribution of the SPI-2 T3SS to infection. Multimutant strains deficient for intracellular replication, for manipulation of host cell defences, or for expression of virulence plasmid effectors all showed strong attenuation *in vivo,* while mutants representing approximately half of the known effector complement showed phenotypes similar to the wild-type parent strain. By additionally removing the SPI-1 T3SS, we find cohorts of effector proteins that contribute to SPI-2 T3SS-driven enhancement of gut inflammation. Further, we provide an example of how iterative mutation can be used to find a minimal number of effector deletions required for attenuation, and thus establish that the SPI-2 effectors SopD2 and GtgE are critical for the promotion of gut inflammation and mucosal pathology. This strategy provides a powerful toolset for simultaneous parallel screening of all known SPI-2 effectors in a single experimental context, and further facilitates the identification of the responsible effectors, and thereby provides an efficient approach to study how individual effectors contribute to disease.

Introduction

A common virulence strategy of Gram-negative pathogens is the use of type-three secretion systems (T3SS) to translocate bacterial effector proteins into host cells (1, 2). Effectors provide a mechanism for the bacterial manipulation of host cells to produce outcomes that favour pathogenesis. *Salmonella enterica* serovars express two distinct T3SS encoded on the genomic regions termed *Salmonella*-pathogenicity island-1 and -2 (SPI-1 and SPI-2) (3). Collectively, effectors translocated by the SPI-1 T3SS mediate invasion into host cells and the induction of a strong inflammatory response in the gut lumen, which diminishes colonisation resistance and promotes expansion of luminal *Salmonella* populations, permitting robust transmission to new hosts (4-6). In contrast, the SPI-2 T3SS is deployed exclusively by intracellular *Salmonella,* which reside within the *Salmonella*-containing vacuole (SCV) in both epithelial cells and phagocytic immune cells (7, 8). SPI-2 effectors contribute to a range of phenotypes that promote intracellular replication and survival, which enables within-host migration to systemic niches and later reseeding of the gut (9, 10). Arguably, the SPI-1 and SPI-2 T3SS together represent the principal virulence factors that mediate the pathogenic lifestyle of *Salmonella*, and indeed a mutant deficient for both T3SS is greatly impaired at inducing gut inflammation, and is not able to efficiently invade into nor survive within host tissue (9, 10). These strong phenotypes should be attributable to the collective functions of translocated effector proteins, in addition to any effect exerted by the injection apparatuses themselves, and so it remains a central challenge to characterise the contribution of individual effectors. While most SPI-1 effectors have clear functions assigned, many SPI-2 effectors remain poorly characterised and it is not clear how individual effectors collectively contribute to the virulence phenotypes mediated by the SPI-2 T3SS.

More than 30 SPI-2 T3SS effectors have been identified for the prototypical laboratory strain *S.* Typhimurium SL1344. Since the discovery and characterisation of the SPI-2 T3SS (7, 8), decades of research has revealed how many of these effectors function to enable SPI-2 virulence, and these efforts are well reviewed elsewhere (11-13). Briefly, SPI-2 effectors collectively contribute to a range of important intracellular activities, including the development and maintenance of the SCV, control of host cell trafficking, manipulation of cell signalling pathways that can lead to pro- or anti-inflammatory outcomes, and interference with the development of adaptive immunity (11, 14). Many SPI-2 effectors are enzymes that catalyse a diverse range of biochemical post-translational modifications to host proteins, while others act in a structural manner by binding to host enzymes to cause changes in substrate specificity (12). The acquisition of a broad complement of effectors over evolutionary time likely contributes to the success of *Salmonella enterica* spp. as a broad host-range pathogen, and similarly represents a highly tuneable bacterial strategy for keeping evolutionary pace with host cell defences that restrict bacterial proliferation. Thus, the study of SPI-2 effectors is critical to understand the mechanisms underpinning bacterial subversion of host cell processes, and should inform better strategies for control of this pathogen.

However, there are significant experimental challenges to the study of individual SPI-2 effectors. Logistically, the creation and characterisation of more than 30 single mutant strains is laborious, and while this strategy has been successful in screening for SPI-2 virulence phenotypes in vitro (15-17), there are significant experimental hurdles in more complicated experimental designs, especially those using animal models of infection. Additionally, many effectors have been reported to have or are speculated to have redundant or interdependent functions. Previous studies exploring single mutant phenotypes have shown that single deletions for most effectors have no impact on intracellular replication or survival during in vitro

experiments (15, 18). The creation of multimutant strains, in which more than one effector is deleted in a particular genetic background, has proven useful in identifying effectors that are necessary or sufficient for certain virulence phenotypes (15, 19, 20). However, in many cases, the design of these multimutants precludes their use in systematically interrogating the function of all effectors in one experimental setup. Thus, there is a need for new tools that enable rapid and logistically simpler interrogation of SPI-2 effector functions, both to understand the activity of individual effectors and to explore how effectors cooperatively or redundantly contribute to broader virulence phenotypes.

Here, we describe the design and construction of six multimutant strains of *S*.Tm SL1344, each deficient for three to six different SPI-2 effectors, collectively covering the known repertoire of SPI-2 effectors in this genetic background. We deployed these mutant strains in several murine models of *Salmonella* infection and found that effector cohorts required for intracellular replication and host-cell survival were critical for expansion in systemic niches, while approximately half of the SPI-2 effector repertoire remained dispensable for virulence. Further, these same effector cohorts were also required for migration from the gut to systemic niches during oral infection. We found that deletion of two effector cohorts could ablate the onset of SPI-2 T3SS-dependent gut inflammation, in the absence of SPI-1 T3SS effector translocation. Finally, we demonstrate a strategy for identifying the individual effectors that contribute to a cohort phenotype by use of simpler mutant strains, and thus describe an unreported role for the effectors SopD2 and GtgE in driving gut inflammation. Together, we show how complex multimutants can be deployed to interrogate virulence phenotypes, a strategy which should be broadly applicable in different experimental contexts.

Results

Construction and validation of SPI-2 effector multimutant strains

To surmount the experimental difficulties in studying how individual SPI-2 effectors contribute to various SPI-2 T3SS-mediated phenotypes, we designed and constructed a set of six multimutant strains in the *Salmonella* Typhimurium (*S.* Tm) SL1344 background. The design of these strains was guided by several criteria: effectors that contribute to similar phenotypes based on their reported functions should be deleted together; each effector should only be deleted once across all six strains; intergenic regions between closely located effectors should be preserved; and effectors should be removed as single deletions where possible, rather than deleting multiple closely-located effectors. The characterisation of SPI-2 effectors has been a priority since the identification and characterisation of the SPI-2 T3SS several decades ago, and thus the depth of literature available permits the loose grouping of effectors into functional groups (**Fig. 1A**). This informed the design of multimutant strains lacking effectors that could reasonably be deleted to produce a strain deficient for a particular function (e.g. a strain lacking several key effectors contributing to development and maintenance of the *Salmonella*-containing vacuole). Some effectors remain poorly characterized with no reported function or host targets, and these were similarly grouped as a multimutant strain. Finally, we used a single mutant deletion for *spvR* to represent a functional deletion of the virulence plasmid-encoded effectors *spvB, spvC,* and *spvD,* in line with previous work (15).

The workflow for generating multimutant strains (**Fig. 1B**) involved the initial construction of single-mutant strains representing all known SL1344 SPI-2 effectors, either by lambda red recombinase-mediated replacement of target genes with antibiotic resistance cassettes, or by leveraging an existing library of single mutant strains constructed in an *S.*Tm 14028S background. These single mutant strains were then used to generate P22 lysates which contained randomly-packaged segments of the bacterial chromosome. Using this library of P22 lysates, we sequentially performed P22 transduction to introduce these gene deletions into a clean SL1344 background, followed by Flp-FRT-mediated removal of resistance cassettes. This process was repeated to sequentially delete up to six genes from an individual strain, and we performed this process in duplicate to generate two independent clone of each multimutant strain. Ultimately, we constructed six multimutant strains covering broad functional groups of *Salmonella* virulence, and assigned these strains designations based on the first six letters of the Greek alphabet (**Fig. 1C**). We performed whole-genome sequencing to validate the construction of these multimutant strains, and to determine the degree of unwanted changes to the chromosome of these strains (**Fig. 1D**). This analysis confirmed that all strains bear the correct deletion based on the intended design, and are thus suitable for experimental use. We detected a number of polymorphisms that likely arose due to successive genetic manipulation and passaging in laboratory conditions, which seemed to loosely correlate to the number of genes deleted in each strain (*i.e.* strains with six deletions tended to bear more polymorphisms than those with four) (**Table S1**). Other polymorphisms are a consequence of transducing genes that were originally deleted in the *S.* Tm 14028 background and transferred to the SL1344 genome (*i.e.* naturally occurring differences in the SL1344 and 14028 genomes) and these are annotated in **Table S1**. We observed distinct polymorphisms arising between two independently constructed clones of each multimutant, suggesting these genetic changes arise randomly during the construction process. This also provides the opportunity to compare the fitness of each clone, to establish whether particular virulence phenotypes may be attributable to these unwanted polymorphisms. Finally, we observed no significant genomic rearrangement or other changes to the genome, including the presence or absence of phages or other mobile elements.

Thus, we report the correct construction of six SPI-2 effector multimutant strains that are suitable for use in various experimental contexts and should be useful in advancing the study of individual and collective SPI-2 effector-mediated phenotypes.

SPI-2 effector cohorts contribute to systemic infection *in vivo*

Next, we aimed to characterise the phenotypes of these multimutant strains in an infection context, and thus describe how different effector cohorts contribute to virulence. We infected C57BL/6 mice with 10^3 *S.* Tm by intraperitoneal injection (**Fig 2A)**, which is a well-established murine model of systemic infection that is characterised by high levels of bacterial replication in systemic niches such as the spleen and liver (21, 22). At day 4 post infection (**Fig 2B**), we observed very high bacterial loads in the liver (left) and spleen (right) of mice infected with *S.*Tm WT, while mice infected with *S.*Tm Δ*ssaV* (deficient for assembly of the SPI-2 T3SS) or *S.*Tm Efl (deficient for all known SPI-2 effectors (15)) had greatly reduced bacterial loads, consistent with the critical role played by the SPI-2 T3SS in mediating intracellular replication and survival. Of the six multimutant strains, we observed a significant reduction in bacterial loads in mice infected with *S.*Tm Alpha, Delta, and Zeta, suggesting the effector groups deleted here play important roles in systemic infection. Surprisingly, three multimutant strains – *S.*Tm Beta, Gamma, and Epsilon – showed bacterial loads to the WT in both liver and spleen, suggesting these effectors are not required for virulence under these conditions. Further, we observed a similar trend in bacterial numbers in the mesenteric lymph node (**Fig S1A**, left), suggesting these effectors play similar roles in colonisation of this site, while colonisation of the gut showed a less clear trend but nonetheless suggests the SPI-2 T3SS is important for delayed gut colonisation, consistent with previous findings (**Fig S1A**, right). To determine if these strong phenotypes arise as a result of bacterial replication and survival, or if these differences are attributable to an initial failure to successfully colonise these sites, we repeated these experiments but euthanised mice at day 2 post infection. We observed a broadly similar trend at this earlier stage of infection (**Fig S1B**) compared to later stages (**Fig 2B, Fig S1A**), which suggests that while these functional cohorts do play distinct roles at early stages, the contribution of these effectors to virulence becomes significantly more pronounced as the systemic infection progresses. Collectively, the systemic infection phenotypes of our SPI-2 effector multimutants are broadly concordant with the reported function of *S.* Tm mutants lacking individual effectors, and so the multimutant phenotypes can be interpreted as compound phenotypes that emerge from the successive deletion of effectors in a given multimutant. Thus, our set of multimutants can provide an efficient means to survey which SPI-2 effectors contribute to a particular virulence phenotype.

A common strategy for studying virulence phenotypes is to perform competitive index experiments, in which a mixed inoculum comprising both the mutant strain and the wild-type strain is used for infection. In animal models of infection, the testing of multiple strains in the same mouse reduces the number of animals required for the analysis, and provides internal controls for animal-specific differences in disease progression. To enable this approach using our multimutant strains, we introduced a unique fitness-neutral genetic tag into each strain (23), alongside the control strains *S.*Tm WT, *S.*Tm Δ*ssaV*, and *S.*Tm Efl. These tags can be quantified with a very high signal-to-noise ratio (greater than 1:100 000), either by quantitative RT-PCR or by a sequence counting utilising PCR amplification and next generation sequencing (24). The resulting collection of 9 tagged strains was then used to infect C57BL/6 mice by i.p. infection (**Fig 2C**) to assay the relative fitness of each strain within a single animal. We observed a similar trend as for single infection (**Fig 2B**) in these mixed infection experiments (**Fig 2D, Fig**

S1C-D), in which *S*.Tm WT, *S*.Tm Beta, *S*.Tm Gamma, and *S*.Tm Epsilon greatly outcompeted *S*.Tm Δ*ssaV, S*.Tm Efl, and the mutant strains *S*.Tm Alpha, *S*.Tm Delta, and *S*.Tm Zeta. These data suggest the deficiencies of effector deletion strains cannot be compensated for by the presence of *S*.Tm WT or other mutants bearing WT-copies of effector genes within the same host animal. As we observed similar phenotypes during single and mixed infection, a mixed inoculum could therefore be used to screen for virulence phenotypes in other experimental contexts in a relatively higher-throughput and logistically simpler manner.

Virulence-dependent migration from the gut to systemic niches

Oral infection represents the natural route of *Salmonella* infection in mice and other animals, and is characterised by invasion into epithelial tissue and induction of a strong inflammatory response in the gut lumen, followed by migration to systemic sites like the spleen and liver which serve as a niche for bacterial replication (3, 25). While the SPI-1 T3SS is the principal virulence factor that mediates gut infection, the SPI-2 T3SS also plays important roles in the colonisation of the lamina propria and a delayed but potent induction of gut inflammation (10, 26). Similarly, there is a strong requirement for SPI-2 T3SS activity in order for *S*.Tm to reach systemic niches beyond the gut. To explore how particular SPI-2 effectors might contribute to these phenotypes, we infected mice (**Fig 3A**) using the well-established streptomycin pre-treatment model of oral infection (10, 27). By day 4 post infection, *S*.Tm WT had colonised (**Fig 3B**) both the liver (left) and spleen (right) and replicated to high numbers, while both *S*.Tm Δ*ssaV* and *S*.Tm Efl were recovered either at very low numbers or not at all, indicating a strong reliance on SPI-2 T3SS virulence for invasive infection of systemic niches. We observed lower population sizes in mice infected with either *S*.Tm Alpha or *S*.Tm Zeta, while *S*.Tm Delta showed an especially pronounced reduction in bacterial load, similar to that observed for *S*.Tm Δ*ssaV* and *S*.Tm Efl. In the mesenteric lymph node (**Fig 3C**), we observed similar colonisation for all strains with modestly reduced CFU for *S*.Tm Δ*ssaV* and *S*.Tm WT Delta. Similarly, we recovered similar numbers in the faeces (**Fig 3D**) of mice infected with each strain, indicating no significant contribution to gut luminal populations as expected for this model (10). Finally, we measured enteropathy in the cecum tissue and observed a broadly similar degree of pathology in all mice (**Fig 3E-F**). While this may suggest a limited contribution of SPI-2 effectors to gut pathology, it seems more likely that the strong pathology induced by the SPI-1 T3SS (10, 27) masks more subtle contributions by SPI-2 effectors. Overall, these data suggest that while there are minimal differences in gut colonisation and tissue pathology between multimutant strains, the subsequent migration to systemic niches followed by intracellular replication and survival is strongly dependent on particular cohorts of SPI-2 effectors, while others remain surprisingly dispensable.

Induction of SPI-2 T3SS-driven gut inflammation requires cohorts of effectors

Using our SPI-2 multimutant strains, we observed relatively little difference in the induction of enteropathy in the cecal tissue (**Fig 3E-F**), which is a hallmark of oral infection in mice and driven largely by the SPI-1 T3SS. We speculated that more subtle contributions of SPI-2 effectors to gut infection, particularly the delayed onset of inflammation, might be masked by the activity of SPI-1 effectors. To explore this, we created a set of SPI-2 multimutant strains that is additionally deficient for SPI-1 T3SS effector translocation by deleting *invG*, encoding a key structural component of the SPI-1 T3SS (28). Thus, these strains are deficient for SPI-1 effector translocation and additionally lack genes for distinct cohorts of SPI-2 effectors, as in **Fig 1C**.

These tools allow for the elucidation of subtle phenotypes that are otherwise undetectable against the severe gut pathology induced by SPI-1 effectors. We performed oral infection in streptomycin pre-treated mice as previously (**Fig 3A)** and observed that both WT and *S*.Tm Δ*invG* are recovered at similar numbers in the liver, spleen, and mesenteric lymph node by day 4 post infection, consistent with previous work (10, 27). Concordantly, there was little difference in CFU recovered for *invG*-deficient multimutants at these sites (**Fig 4A**) compared to the respective *invG*-competent strains (**Fig 3B-C**). This suggests that SPI-2 remains the primary virulence factor mediating colonisation of systemic sites. By day 4 post infection, we observed a trend towards reduced faecal loads for *S*.Tm Δ*invG*Δ*ssaV* (deficient for both SPI-1 and SPI-2 T3SS assembly), consistent with previous reports (29). Interestingly, a similar trend was observed for all *invG*-deficient multimutants (**Fig 4B**), perhaps suggesting previously unidentified roles for diverse SPI-2 T3SS effectors in the prolongation of *S*. Tm gut colonisation.

Induction of gut inflammation mediated by the SPI-1 T3SS is a well-established hallmark of infection in the streptomycin pre-treatment model, while SPI-1 mutants cause delayed but significant inflammation in a SPI-2 T3SS-dependent manner (26). While the mechanisms of SPI-2 driven inflammation remain enigmatic, this delayed inflammation has been linked to prolonged *S*.Tm gut colonisation (10, 29-31). Here, we also observed a gradual but strong increase in gut inflammation in the *S*.Tm Δ*invG* strain (thus caused by SPI-2 effectors), while *S*.Tm Δ*invG*Δ*ssaV* strain fails to induce gut inflammation, as expected (**Fig 4C**). For most *invG*-deficient multimutants we observed a similar trend in which initially uninflamed conditions in the gut gave rise to potent inflammation by day 4 post infection, based on lipocalin-2 ELISA. However, we noted a previously unappreciated trend in which no multimutant produced inflammation to the degree of the SPI-1 or SPI-2 competent strains, which may suggest that diverse perturbations of the SPI-2 effector complement can disrupt the induction of gut inflammation. Regardless, we observed particularly strong phenotypes for *S*.Tm Alpha and *S*.Tm Delta, which showed inflammation profiles similar to that of *S*.Tm Δ*invG*Δ*ssaV* and greatly diminished relative to *S*.Tm WT (**Fig 4C**). To further explore the contributions to gut pathology, we repeated our examination of cecal pathology in these mice (**Fig 4D-E**). Here, we observed that both *S*.Tm Δ*invG* and *S*.Tm Δ*ssaV* could produce enteropathy that contributes to the strong level of disease seen in *S*.Tm WT-infected mice, while mice infected with *S*.Tm Δ*invG*Δ*ssaV* retained relatively healthy gut tissue. This healthy state was phenocopied by both *S*.Tm *invG* Alpha and *S*.Tm *invG* Delta, suggesting that in the absence of the SPI-1 T3SS these effector cohorts contribute to potent SPI-2-dependent gut inflammation and pathology. All other *invG*-deficient multimutants produced enteropathy approaching that of the control strains, indicating a dispensability of the induction of gut pathology. Together, these data provide initial mechanistic insights into how SPI-2 effectors can contribute to delayed but significant inflammatory phenotypes in the intestinal mucosa.

Iterative deletion of effector genes reveals individual SPI-2 effectors required for gut inflammation

As described in **Fig 1C**, the multimutant strains were constructed via sequential deletion of individual effector genes. Thus, the creation of a six-fold mutant required the preceding construction of the parent five-fold mutant, and before that a four-fold mutant, *et cetera*. Each stepwise mutant was preserved in cryostorage, and thus it is possible to use these simpler mutants to determine which particular genes may contribute to the phenotype observed for the complete multimutant. To provide an example of this strategy, we chose to focus on the *S*.Tm Delta strain, which we showed was deficient for colonisation of systemic niches during

intraperitoneal infection (**Fig 2**), and showed pronounced attenuation for migration from the gut to these systemic niches in oral infection (**Fig 3**), and was ultimately shown to contribute to SPI-2-dependent gut inflammation and enteropathy (**Fig 4**). The *S*.Tm Delta mutant comprises deletions in four effector genes: *steC, sseL, sopD2,* and *gtgE*. To determine which effectors contribute to the strong phenotype observed for this multimutant, we used the Δ*steC*Δ*sseL* double mutant created during the stepwise construction of *S*.Tm Delta, and separately constructed a Δ*sopD2*Δ*gtgE* double mutant. We infected mice by oral gavage as previously (**Fig 3A**), and observed that *S*.Tm Δ*steC*Δ*sseL* phenocopied *S*.Tm WT, while the Δ*sopD2*Δ*gtgE* double mutant was recovered in similar numbers to *S*.Tm Δ*ssaV* (**Fig 5A, Fig S2A**), and thus these two effectors alone mediate the *S*.Tm Delta phenotypes. We next used single mutants to determine the relative contribution of each individual effector, and found only partial reductions relative to the WT, demonstrating that both effectors must be deleted together to produce this phenotype, likely due to the functional overlap between these effectors. Finally, we complemented the Δ*sopD2*Δ*gtgE* double mutant by sequential chromosomal restoration of WT copies of these genes, and found that the double-complemented Δ*sopD2*Δ*gtgE* mutant was restored to approximately WT levels in this infection model (**Fig 5A, Fig S2A**). Thus, we demonstrate how complex multimutant phenotypes can be interrogated by characterising simpler mutants in a deductive manner,

Previous work has described how SopD2 and GtgE are critical for systemic proliferation following intraperitoneal injection of mice (32), but the contributions of these effectors to gut pathology remains unexplored. Here, we established that gut inflammation during oral infection could be ablated by deletion of both the SPI-1 T3SS and certain cohorts of SPI-2 effectors, including those deficient in *S*.Tm Delta (**Fig 4D-E**). Given that deletion of *sopD2* and *gtgE* was sufficient to phenocopy *S*.Tm Delta in terms of systemic colonisation (**Fig 5A)**, we hypothesised that deletion of these two effectors and the SPI-1 T3SS would similarly be sufficient to reduce gut inflammation to levels seen for the avirulent *S*.Tm Δ*invG*Δ*ssaV*. To explore this, we deleted *invG* from the double mutant *S*.Tm Δ*sopD2*Δ*gtgE* and orally infected mice as previously (**Fig 3A**). Indeed, while a triple mutant *S*.Tm Δ*invG*Δ*sopD2*Δ*gtgE* failed to successfully colonise the liver, spleen, and mesenteric lymph nodes in a manner similar to the double mutant *S*.Tm Δ*sopD2*Δ*gtgE* (**Fig 5B**), there was a marked decrease in gut inflammation whereby the triple mutant failed to induce both early and late stage inflammation, similar to levels seen for the avirulent Δ*invG*Δ*ssaV* strain (**Fig 5C**, **Fig S2B**).

Intracellular reservoirs of *S*.Tm residing in the cecal tissue can contribute to sustained gut pathology (10, 33). We performed a gentamycin protection assay on infected mucosal tissue (34) to determine the contribution of SopD2 and GtgE to survival of intracellular *S*.Tm within cecal tissue. Here, we recovered fewer *S*.Tm Δ*invG*Δ*sopD2*Δ*gtgE* and *S*.Tm Δ*invG*Δ*ssaV* relative to *S*.Tm WT (**Fig 5D**), perhaps suggesting local replication and survival in cecal tissue is important for sustained gut inflammation. Finally, we discovered a corresponding ablation of enteropathy in the cecum of mice infected with either *S*.Tm Δ*invG*Δ*sopD2*Δ*gtgE* or Δ*invG*Δ*ssaV*, confirming that deletion of these two SPI-2 effectors is sufficient for ablation of SPI-2 T3SS-dependent gut inflammation (**Fig 5E-F**). Collectively, these data provide new mechanistic insights into how specific SPI-2 effectors contribute to inflammatory outcomes in the infected gut, and provide a proof of concept for how strong phenotypes observed using *S*.Tm effector multimutant strains can be rapidly narrowed to candidate effectors responsible for this activity (**Fig 6**).

Discussion

The intracellular lifestyle of pathogenic *Salmonella enterica* spp. is driven by the activity of SPI-2 T3SS effectors, but efforts to characterise the function of individual effectors have proven complicated, either by instances of interdependency or redundancy between effectors, or by the logistical difficulties in characterising more than 30 proteins across different experimental contexts. Here, we designed SPI-2 effector multimutants to explore which effector cohorts are critical for pathogenesis in a logistically easier manner, and showed how such tools can be used to find a minimal set of effectors responsible for key phenotypes, using SPI-2-dependent promotion of gut inflammation as an example.

In designing and constructing SPI-2 effector multimutants, we loosely grouped effectors that reportedly contribute to similar functions. For example, the six effectors deleted in *S*.Tm Alpha (*sseF, sseG, sifA, sseJ, pipB2, steA*) collectively contribute to development and maintenance of the SCV, while *S*.Tm Beta is deficient for six effectors (*sseK1, sseK2, sseK3, gtgA, gogA, pipA*) that antagonise different aspects of host cell signalling pathways. The rational grouping of deletions is dependent on the reported function of each effector (**Fig 1A**), and many effectors have functions that are unknown or disputed. Thus, it is possible that unreported functions or inter-effector relationships may contribute to phenotypes that are masked by the current design. Similarly, undiscovered effectors likely exist and the activity of those effectors may contribute to shared phenotypes. While we observed strong phenotypes for several multimutants (*S*.Tm Alpha, Delta, and Zeta), other mutants (*S*.Tm Beta, Gamma, and Epsilon) representing approximately half of the known SL1344 effector repertoire phenocopied *S*.Tm WT in different infection models. It is possible that these effectors do have phenotypes in other infection models (e.g. in a different host species, or during chronic infection), or that the impact is too subtle to measure via the methods used here. Ultimately, further careful characterisation of these mutants in different infectious contexts and using different methodology will be useful to fully characterise the role of these effectors. An alternative explanation for the lack of strong phenotypes for several mutants tested here is the context-dependency of deletion mutants, described elsewhere as the effector network hypothesis (35-37). Effectors of the gut pathogen *Citrobacter rodentium* reportedly form robust networks that can tolerate the loss of a number of effectors, but deletion of an increasingly large number of effectors ultimately causes a collapse of virulence phenotypes back to an avirulent level. Importantly, this same study describes context-dependent essentiality of effectors, in which deletion of a single effector may or may not produce a strong phenotype depending on the availability of other effectors (35). Certainly this possibility may also exist for the effector cohort of *S*.Typhimurium, and this may complicate the comparison of studies such as ours with previous and future work.

Other studies have employed the strategy of sequentially deleting multiple genes encoding effector proteins, though the design and rationale for these efforts varies. Chen *et al* (15) iteratively deleted the majority of known SPI-2 effectors in a single genetic background, producing an 'effectorless' *S*. Tm SL1344 derivative that is otherwise competent for SPI-2 T3SS assembly and function. Restoring selected effectors to this effectorless strain by complementation allowed for the identification of a 'minimal network' of effectors that was sufficient for virulence during oral infection *(sifA*, *sseFG*, *steA*, *sopD2*, and *spvBCD*) (15). Elsewhere, separate studies have focused on deleting core sets of effectors to produce a strain that is reduced to Δ*ssaV*-levels of virulence. Strong phenotypes have thus been reported for a seven-fold deletion strain (*S*.Tm Δ*sseF* Δ*sseG* Δ*sifA* Δ*sopD2* Δ*sseJ* Δ*steA* Δ*pipB2*) (19), and separately for a five-fold deletion (*S*.Tm Δ*sifA* Δ*spvB* Δ*sseF* Δ*sseJ* Δ*steA*, created in a SPI-1 T3SS-deficient background) (20). These efforts represent important steps in understanding how

individual effectors contribute to strong collective phenotypes, but they are less useful in contexts where screening for individual effectors is important. The advantage of our strategy described here is that the activity of all effectors can be explored in a single experimental context, and responsible effectors can subsequently be identified by use of simpler mutants. We anticipate that these multimutant strains could be used to screen for SPI-2 T3SS effector functions in other experimental contexts and infection models, for example to study chronic carriage in genetically resistant mice, intracellular replication *in vitro* in various host cell types, virulence phenotypes in various genetically-modified mouse backgrounds, or performance in reporter assays that measure cell signalling outcomes.

Our work highlights the strong contribution of SopD2 and GtgE to virulence in both oral and systemic infection. The molecular target of both of these effectors is the host GTPase Rab32 (32, 38), which restricts intracellular bacteria via its nucleotide exchange factor BLOC-3 (39). The acquisition of SopD2 and GtgE by *S*.Typhimurium permits the complementary antagonism of Rab32, in which SopD2 functions as a GAP mimic to limit Rab32 GTPase activity, while GtgE directly proteolytically cleaves Rab32 (32, 38). In the absence of these effectors, Rab32 and the co-factor BLOC-3 facilitate the delivery of itaconate to the SCV (40, 41), which restricts intravacuolar *S*.Tm by metabolic disruption of the glyoxylate shunt and thereby reduces bacterial replication (42). Thus, effector-mediated disruption of the Rab32-BLOC-3-itaconate axis represents an important strategy for the success of intracellular *S*.Tm populations. While it had been established that SopD2 and GtgE were important for promoting intracellular survival in systemic niches (32), the contributions of these effectors to gut pathology and inflammation remained unknown.

Here, we show that *S*.Tm Delta and *S*.Tm Δ*sopD2*Δ*gtgE* cannot reach systemic niches following oral infection (**Fig 3**), and this mutant also show severe attenuation in systemic sites during intraperitoneal infection (**Fig 2**), similar to *S*.Tm Δ*ssaV* (10, 26). Given that itaconate-mediated disruption of intracellular *S*.Tm restricts actively replicating bacteria (42), this may suggest that bacterial replication is an important activity for successful migration from the gut to systemic niches, or that cell-intrinsic host defenses impose particularly stringent control of intracellular bacteria during these migration events or during subsequent bacterial growth in systemic niches. Importantly, our current work extends previous knowledge by discovering a previously unknown function of SopD2 and GtgE in eliciting mucosal inflammation in a SPI-1 T3SS-deficient background (**Fig 4C-E**, **Fig 5B-F**). This finding will enable future work at molecular and cellular scales to explore why the *S*.Tm Δ*invG*Δ*sopD2*Δ*gtgE* mutant is drastically impaired at inducing gut inflammation (**Fig 5C, Fig 5E-F**). It may be that a reduction of bacterial numbers in the gut tissue causes a corresponding impairment of gut inflammation, but we observed only a modest reduction in CFU in the mesenteric lymph node (**Fig 5B**) and faeces (**Fig S2B**), and similarly a slight reduction in the intracellular population within caecal tissue (**Fig 5D**). Future work should focus on the molecular mechanisms that underpin how SopD2 and GtgE promote *S.* Tm growth and survival in the gut, on how this affects inflammation and mucosal pathology, and on how host cell defences (*e.g.* itaconate) prevent pathogen migration to systemic sites.

While we observed the strongest deficiency for *S*.Tm Delta, we also found that both *S*.Tm Alpha and *S*.Tm Zeta were significantly reduced in the liver and spleen during both oral (**Fig 3**) and systemic infection models (**Fig 2**). We observed that *S*.Tm Alpha colonised these sites at approximately *S*.Tm Δ*ssaV* levels by day 2 post infection, then increased modestly in the following days, suggesting this mutant can still replicate intracellularly to some extent, despite lacking the principal effectors mediating SCV maturation and expansion. Alternatively, it may be possible that this increase is attributable to extra-vacuolar or extracellular replication, or to cell-

to-cell spread via efferocytosis or simply bacterial egress and reinvasion (43-45). Future work, especially using *in vitro* models of infection, will be useful to determine the replicative defect of this strain. We observed that *S*.Tm Alpha Δ*invG* was greatly attenuated at inducing mucosal inflammation by day 4 post infection, similar to S.Tm Delta Δ*invG*, and this is consistent with previous work linking some of these effectors to gut inflammation (20). Future work is needed to understand which minimal subset of effectors contribute to this activity, and to understand how effectors responsible for intracellular replication contribute to the induction of gut inflammation. Separately, we observed a similarly strong phenotype for *S*.Tm Zeta, which is deficient for the regulator SpvR and thus impaired for expression of genes on the virulence plasmid regulon *spvABCD* (46, 47). Effectors on this operon reportedly have a range of functions: SpvB is an ADP-ribosyltransferase which causes disruption to the host cytoskeleton and also promotes cell death via apoptosis (48-50); SpvC has anti-inflammatory functions via its phosphothreonine lyase activity against several MAPK signalling proteins (51-53); while SpvD acts as a cysteine protease to inhibit NF-kB signalling, possibly by targeting host exportin Xpo2 (54, 55). In this study, we show that *S*.Tm Zeta is strongly attenuated at colonising systemic niches but remains competent for inducing SPI-2 T3SS-dependent gut inflammation, which suggests these activities are not necessarily linked, but further work is needed to understand how the reported molecular activities of these proteins contributes to these disease phenotypes.

In conclusion, we describe how multimutants created by sequential deletion of functionally linked genes can be easily used in a variety of experimental contexts to gain new insights into bacterial virulence. We show that effector cohorts linked to intracellular replication and protection from host cell defenses are important for migration from the gut to systemic niches, and these same cohorts also contribute to SPI-2 T3SS-dependent gut inflammation. Finally, we show that the effectors SopD2 and GtgE together are necessary for these phenotypes, providing new insights into how the SPI-2 T3SS contributes to gut infection and migration within the host. We anticipate that these multimutants will prove useful in other experimental contexts to provide new insights into bacterial virulence strategies.

Methods

Strains used in this study

All bacterial strains used in this study were *S.* Tm SL1344 SB300 (56) or derivatives and are listed in **Table 1**. Strains in cryostorage at -80 °C were streaked to selective media and subsequently used to inoculate overnight cultures comprising lysogeny broth (LB) medium containing appropriate antibiotics (50 µg/ml streptomycin, 50 µg/ml ampicillin, 50 µg/ml kanamycin, or 15 µg/ml chloramphenicol, as required).

Strain construction

All primers used for strain construction and validation are listed in **Table 2**. Single mutant strains were constructed using the lambda-red protocol, in which a gene of interest is replaced with an antibiotic resistance cassette flanked by FRT sites (57). Primers were designed with approximately 40 base pairs flanking the gene of interest and 20 base pairs of an antibiotic resistance cassette. Plasmids pKD3 or pKD4 were used as DNA templates in PCR reactions to amplify products suitable for gene replacement with cassettes encoding chloramphenicol (pKD3) or kanamycin (pKD4) resistance via homologous recombination. *S.*Tm SL1344 carrying the plasmid pKD46 was incubated for 3 hours at 30 °C in LB containing 50 µg/ml ampicillin and 10 mM arabinose. Cells were washed in ice cold water and concentrated via centrifugation, then transformed with purified DNA via electroporation. Cells were let to recover in LB for 1 hour at 37°C, then plated to LB agar plates containing either 50 µg/ml kanamycin or 15 µg/ml chloramphenicol, as required. Colonies were picked and genotyped via PCR with primers flanking the replaced gene of interest. P22 lysates were generated from these mutant strains, and used to transfer the deletion of interest to a clean strain of *S.*Tm SL1344, which was subsequently passaged via replating several times to promote clearance of phage and re-genotyped via PCR. Multimutants were similarly constructed by repeated rounds of P22 transduction as above. Strains bearing both chloramphenicol and kanamycin resistance (*i.e.* after two rounds of P22 transduction) had these resistance cassettes removed via electroporation with pCP20 encoding the *Flp* recombinase flippase. All strains were re-genotyped after each round of Flp-FRT recombination, to avoid unwanted recombination events at FRT scar sites.

Chromosomal complementation of effector genes

Mutant strains deficient for *sopD2* and *gtgE* were complemented with these genes via subcloning into a suicide vector followed by conjugation and homologous recombination into recipient strains. Briefly, PCR was used to generate amplicons comprising either *sopD2* or *gtgE* with 1000 bp flanking regions and suitable restriction sites. Amplicons were cloned into vector pSB890 via T4 DNA ligase reactions, then used to transform electrocompetent *E. coli* SM10λpir. Overnight cultures of recipient strains were prepared, then combined with cultures of donor strains. Selection with sucrose and tetracycline was used to identify successful conjugation and recombination events, which were confirmed by genotyping PCR.

Whole-genome sequencing and bioinformatics analysis

Overnight cultures of multimutant strains were pelleted by centrifugation and genomic DNA was extracted using a QIAmp DNA Mini Kit (Qiagen) according to the manufacturer's instructions. Library preparation and short-read Illumina sequencing were performed by BMKGENE to confirm deletion of target genes and assess the degree of other polymorphisms in the genome. The resulting raw reads were cleaned by removing adaptor sequences, low-quality-end trimming and removal of low-quality reads using BBTools v 38.18 using the parameters trimq = 14, maq = 20, maxns = 0 and minlength = 45. (Bushnell, B. BBMap. Available from: https://sourceforge.net/projects/bbmap/.). The genetic changes in the strains as compared to the reference genome (GCF_000210855.2) were identified using breseq (v. 0.38) run in consensus mode with default parameters (58). Sequencing data is available from the European Nucleotide Archive (ENA) using the accession number PRJEB83585.

Animal husbandry

Animal experiments were conducted in accordance with the Swiss Federal Government guidelines in animal experimentation law (SR 455.163 TVV). Protocols used were approved by the Cantonal Veterinary Office of the canton Zurich, Switzerland (Kantonales Veterinäramt ZH licenses 108/2022, 109/2022, 158/2019, 193/2016). Animals were bred and kept under specific pathogen free conditions in individually ventilated cages (EPIC and RCHCI facilities, ETH Zurich). Wild-type C57BL/6J mice were used for all *in vivo* experiments described here. Mice were aged 8-10 weeks at the start of experiments, and a balanced number of males and females was used. Mice were monitored daily and scored for health status in a range of criteria per animal licence requirements, and euthanised prior to experimental endpoint if necessary.

Animal infection experiments

Mice were infected and treated following the experimental schemes described in each figure and corresponding figure legend. For infections requiring intraperitoneal injection, overnight cultures were incubated on a rotating wheel at 37 °C for 12 hours. Overnight cultures were washed in PBS then diluted to achieve approximately 10^4 CFU/ml. For single infections (**Fig 2B**), mice received 100 µl of this washed solution by intraperitoneal injection giving an infectious dose of approximately 10^3 CFU. For mixed infections (**Fig 2D**), mice received 100 µl of washed solution to achieve an inoculum of 10^3 CFU comprising equivalent volumes of each strain, as required. For infections requiring oral gavage (**Fig 3-5**), mice were gavaged with 25mg streptomycin one day prior to infection. Overnight cultures were used to inoculate subcultures which were incubated on a rotating wheel at 37 °C for 4 hours. Subcultures were washed in PBS then aliquoted to prepare inocula comprising approximately $5x10^7$ CFU in a 50 µl volume, which was delivered to the mice by oral gavage. Faeces was collected in pre-weighed tubes containing 1 ml PBS and homogenised with a steel ball for 2 minutes at 25 Hz using a Tissue-Lyser (Qiagen). Mice were euthanised at indicated time-points, and organs were aseptically removed. CFU per organ was quantified by plating to MacConkey agar containing 50 ug / ml streptomycin. Data for liver, spleen, and mesenteric lymph node is presented as CFU per organ, while data for faeces is presented as CFU per gram of faeces.

Measurement of genomic barcodes by qPCR

Overnight cultures were inoculated with homogenates of indicated organs to enrich for bacterial genetic material, comprising 100 µl homogenate in 2 ml LB and appropriate antibiotics. Cultures were incubated for 12 hours at 37 °C on a rotating wheel. Overnight cultures were pelleted by centrifugation and genomic DNA was extracted using a QIAmp DNA Mini Kit (Qiagen) according to the manufacturer's instructions. The abundance of each genetic tag was measured by qPCR as described previously (59). Relative proportions of each tag were calculated by dividing the DNA copy number of each tag by the sum of all tags within a sample.

Histology

Tissue samples were embedded in O.C.T. (Sakura), snap-frozen in liquid nitrogen, and stored at -80 °C. Cryosections were prepared at 5 µm width and mounted on glass slides, then stained with hematoxylin and eosin (H&E). Pathological evaluation was performed in a blinded manner based on the criteria described previously (27). Briefly, samples were scored on four criteria: degree of submusocal edema; infiltration of polymorphonuclear granulocytes into the lamina propria; number of goblet cells; and integrity of the epithelia. Scores for each category were combined to achieve a total score representing the pathological state of each sample.

Lipocalin-2 ELISA

Homogenised faecal samples were thawed from storage at -20 °C and centrifuged to remove faecal material. Lipocalin-2 levels in the supernatant were quantified using a Lipocalin-2 ELISA kit (R & D Systems) according to the manufacturer's instructions. All samples were analysed in duplicate at three different dilutions (undiluted, 1:20, and 1:400), and concentrations were determined by four parameter logistic regression curve.

Gentamicin protection assay for cecal tissue

Cecal tissue was aseptically extracted from mice following euthanisation, and incubated for 30 minutes in PBS containing 400 µg/ml gentamicin to kill extracellular bacteria. Tissue was then washed rigorously six times in PBS, then homogenised with a steel ball for 2 minutes at 25 Hz using a Tissue-Lyser (Qiagen). CFU was quantified by plating to MacConkey agar containing 50 ug / ml streptomycin.

Statistical analysis and software

GraphPad Prism was used to perform statistical tests and generate graphs. Where applicable, statistical significance was assessed by Mann-Whitney *U* test, as described in figure legends. BioRender was used to generate some graphical elements, including experimental schemes and **Fig 6**. Figures were assembled in Abode Illustrator.

Acknowledgements

The authors would like to thank members of the Hardt lab for productive discussion and for technical support. We would like to thank the staff at RCHCI and EPIC animal facilities, and the staff at the Institute of Microbiology at ETH Zurich for their support.

Funding

This work has been funded by grants from the Swiss National Science Foundation (310030B_173338/1, 310030_192567, 10.001.588) to WDH, and also supported by the NCCR Microbiomes, funded by the Swiss National Science Foundation (51NF40_180575; to SS and WDH). JPMN was supported by a Swiss Government Excellence Scholarship (2019.0843). NMA was funded by the National Institute of Health (AI083359) and The Welch Foundation (I-1704).

Contributions

J.P.M.N., F.G., P.P., A.M., S.M., and W.D.H. conceived and designed the experiments. J.P.M.N., F.G., P.P., A.M., A.S., M.B., Y.S., S.M., and U.E. performed the experiments. All authors contributed to data analysis and writing of the manuscript.

References

1. Galan JE, Waksman G. 2018. Protein-Injection Machines in Bacteria. Cell 172:1306-1318.
2. Deng W, Marshall NC, Rowland JL, McCoy JM, Worrall LJ, Santos AS, Strynadka NCJ, Finlay BB. 2017. Assembly, structure, function and regulation of type III secretion systems. Nat Rev Microbiol 15:323-337.
3. Han J, Aljahdali N, Zhao S, Tang H, Harbottle H, Hoffmann M, Frye JG, Foley SL. Infection biology of Salmonella enterica. EcoSal Plus 0:eesp-0001-2023.
4. Galán JE, Curtiss R, 3rd. 1989. Cloning and molecular characterization of genes whose products allow Salmonella typhimurium to penetrate tissue culture cells. Proc Natl Acad Sci U S A 86:6383-7.
5. Galán JE. 2021. Salmonella Typhimurium and inflammation: a pathogen-centric affair. Nature Reviews Microbiology 19:716-725.
6. Fattinger SA, Sellin ME, Hardt WD. 2021. Salmonella effector driven invasion of the gut epithelium: breaking in and setting the house on fire. Curr Opin Microbiol 64:9-18.
7. Shea JE, Hensel M, Gleeson C, Holden DW. 1996. Identification of a virulence locus encoding a second type III secretion system in Salmonella typhimurium. Proc Natl Acad Sci U S A 93:2593-7.
8. Hensel M, Shea JE, Gleeson C, Jones MD, Dalton E, Holden DW. 1995. Simultaneous identification of bacterial virulence genes by negative selection. Science 269:400-3.
9. Maier L, Diard M, Sellin ME, Chouffane ES, Trautwein-Weidner K, Periaswamy B, Slack E, Dolowschiak T, Stecher B, Loverdo C, Regoes RR, Hardt WD. 2014. Granulocytes impose a tight bottleneck upon the gut luminal pathogen population during Salmonella typhimurium colitis. PLoS Pathog 10:e1004557.
10. Hapfelmeier S, Stecher B, Barthel M, Kremer M, Muller AJ, Heikenwalder M, Stallmach T, Hensel M, Pfeffer K, Akira S, Hardt WD. 2005. The Salmonella pathogenicity island (SPI)-2 and SPI-1 type III secretion systems allow Salmonella serovar typhimurium to trigger colitis via MyD88-dependent and MyD88-independent mechanisms. J Immunol 174:1675-85.
11. LaRock DL, Chaudhary A, Miller SI. 2015. Salmonellae interactions with host processes. Nat Rev Microbiol 13:191-205.
12. Pillay TD, Hettiarachchi SU, Gan J, Diaz-Del-Olmo I, Yu XJ, Muench JH, Thurston TLM, Pearson JS. 2023. Speaking the host language: how Salmonella effector proteins manipulate the host. Microbiology (Reading) 169.
13. Jennings E, Thurston TLM, Holden DW. 2017. Salmonella SPI-2 Type III Secretion System Effectors: Molecular Mechanisms And Physiological Consequences. Cell Host Microbe 22:217-231.
14. Haraga A, Ohlson MB, Miller SI. 2008. Salmonellae interplay with host cells. Nat Rev Microbiol 6:53-66.
15. Chen D, Burford WB, Pham G, Zhang L, Alto LT, Ertelt JM, Winter MG, Winter SE, Way SS, Alto NM. 2021. Systematic reconstruction of an effector-gene network reveals determinants of Salmonella cellular and tissue tropism. Cell Host & Microbe 29:1531-1544.e9.
16. Bayer-Santos E, Durkin CH, Rigano LA, Kupz A, Alix E, Cerny O, Jennings E, Liu M, Ryan AS, Lapaque N, Kaufmann SHE, Holden DW. 2016. The Salmonella Effector SteD Mediates MARCH8-Dependent Ubiquitination of MHC II Molecules and Inhibits T Cell Activation. Cell Host & Microbe 20:584-595.
17. Stapels DAC, Hill PWS, Westermann AJ, Fisher RA, Thurston TL, Saliba AE, Blommestein I, Vogel J, Helaine S. 2018. Salmonella persisters undermine host immune defenses during antibiotic treatment. Science 362:1156-1160.
18. Buckner MMC, Croxen M, Arena ET, Finlay BB. 2011. A comprehensive study of the contribution of Salmonella enterica serovar Typhimurium SPI2 effectors to bacterial

colonization, survival, and replication in typhoid fever, macrophage, and epithelial cell infection models. Virulence 2:208-216.

19. Knuff-Janzen K, Tupin A, Yurist-Doutsch S, Rowland JL, Finlay BB. 2020. Multiple Salmonella-pathogenicity island 2 effectors are required to facilitate bacterial establishment of its intracellular niche and virulence. PLOS ONE 15:e0235020.
20. Matsuda S, Haneda T, Saito H, Miki T, Okada N. 2019. Salmonella enterica Effectors SifA, SpvB, SseF, SseJ, and SteA Contribute to Type III Secretion System 1-Independent Inflammation in a Streptomycin-Pretreated Mouse Model of Colitis. Infect Immun 87.
21. Shea JE, Beuzon CR, Gleeson C, Mundy R, Holden DW. 1999. Influence of the Salmonella typhimurium pathogenicity island 2 type III secretion system on bacterial growth in the mouse. Infect Immun 67:213-9.
22. Lawley TD, Chan K, Thompson LJ, Kim CC, Govoni GR, Monack DM. 2006. Genome-wide screen for Salmonella genes required for long-term systemic infection of the mouse. PLoS Pathog 2:e11.
23. Daniel BBJ, Steiger Y, Sintsova A, Field CM, Nguyen BD, Schubert C, Cherrak Y, Sunagawa S, Hardt WD, Vorholt JA. 2024. Assessing microbiome population dynamics using wild-type isogenic standardized hybrid (WISH)-tags. Nat Microbiol 9:1103-1116.
24. Sintsova A, Ruscheweyh HJ, Field CM, Feer L, Nguyen BD, Daniel B, Hardt WD, Vorholt JA, Sunagawa S. 2024. mBARq: a versatile and user-friendly framework for the analysis of DNA barcodes from transposon insertion libraries, knockout mutants, and isogenic strain populations. Bioinformatics 40.
25. Nguyen AT, McSorley SJ. 2024. Fighting the enemy within: Systemic immune defense against mucosal Salmonella infection. Immunol Lett 270:106930.
26. Coburn B, Li Y, Owen D, Vallance BA, Finlay BB. 2005. Salmonella enterica serovar Typhimurium pathogenicity island 2 is necessary for complete virulence in a mouse model of infectious enterocolitis. Infect Immun 73:3219-27.
27. Barthel M, Hapfelmeier S, Quintanilla-Martinez L, Kremer M, Rohde M, Hogardt M, Pfeffer K, Russmann H, Hardt WD. 2003. Pretreatment of mice with streptomycin provides a Salmonella enterica serovar Typhimurium colitis model that allows analysis of both pathogen and host. Infect Immun 71:2839-58.
28. Kaniga K, Bossio JC, Galán JE. 1994. The Salmonella typhimurium invasion genes invF and invG encode homologues of the AraC and PulD family of proteins. Mol Microbiol 13:555-68.
29. Stecher B, Robbiani R, Walker AW, Westendorf AM, Barthel M, Kremer M, Chaffron S, Macpherson AJ, Buer J, Parkhill J, Dougan G, von Mering C, Hardt WD. 2007. Salmonella enterica serovar typhimurium exploits inflammation to compete with the intestinal microbiota. PLoS Biol 5:2177-89.
30. Diard M, Garcia V, Maier L, Remus-Emsermann MN, Regoes RR, Ackermann M, Hardt WD. 2013. Stabilization of cooperative virulence by the expression of an avirulent phenotype. Nature 494:353-6.
31. Gül E, Bakkeren E, Salazar G, Steiger Y, Abi Younes A, Clerc M, Christen P, Fattinger SA, Nguyen BD, Kiefer P, Slack E, Ackermann M, Vorholt JA, Sunagawa S, Diard M, Hardt WD. 2023. The microbiota conditions a gut milieu that selects for wild-type Salmonella Typhimurium virulence. PLoS Biol 21:e3002253.
32. Spanò S, Gao X, Hannemann S, Lara-Tejero M, Galán JE. 2016. A Bacterial Pathogen Targets a Host Rab-Family GTPase Defense Pathway with a GAP. Cell Host Microbe 19:216-26.
33. Dolowschiak T, Mueller AA, Pisan LJ, Feigelman R, Felmy B, Sellin ME, Namineni S, Nguyen BD, Wotzka SY, Heikenwalder M, von Mering C, Mueller C, Hardt WD. 2016. IFN-gamma Hinders Recovery from Mucosal Inflammation during Antibiotic Therapy for Salmonella Gut Infection. Cell Host Microbe 20:238-49.
34. Fattinger SA, Bock D, Di Martino ML, Deuring S, Samperio Ventayol P, Ek V, Furter M, Kreibich S, Bosia F, Muller-Hauser AA, Nguyen BD, Rohde M, Pilhofer M, Hardt WD,

Sellin ME. 2020. Salmonella Typhimurium discreet-invasion of the murine gut absorptive epithelium. PLoS Pathog 16:e1008503.

35. Ruano-Gallego D, Sanchez-Garrido J, Kozik Z, Nunez-Berrueco E, Cepeda-Molero M, Mullineaux-Sanders C, Naemi-Baghshomali Clark J, Slater SL, Wagner N, Glegola-Madejska I, Roumeliotis TI, Pupko T, Fernandez LA, Rodriguez-Paton A, Choudhary JS, Frankel G. 2021. Type III secretion system effectors form robust and flexible intracellular virulence networks. Science 371.
36. Sanchez-Garrido J, Alberdi L, Chatterjee S, Frankel G, Mullineaux-Sanders C. 2021. Type III secretion system effector subnetworks elicit distinct host immune responses to infection. Curr Opin Microbiol 64:19-26.
37. Sanchez-Garrido J, Ruano-Gallego D, Choudhary JS, Frankel G. 2022. The type III secretion system effector network hypothesis. Trends Microbiol 30:524-533.
38. Spanò S, Galán JE. 2012. A Rab32-dependent pathway contributes to Salmonella typhi host restriction. Science 338:960-3.
39. Gerondopoulos A, Langemeyer L, Liang J-R, Linford A, Barr Francis A. 2012. BLOC-3 Mutated in Hermansky-Pudlak Syndrome Is a Rab32/38 Guanine Nucleotide Exchange Factor. Current Biology 22:2135-2139.
40. Chen M, Sun H, Boot M, Shao L, Chang SJ, Wang W, Lam TT, Lara-Tejero M, Rego EH, Galán JE. 2020. Itaconate is an effector of a Rab GTPase cell-autonomous host defense pathway against Salmonella. Science 369:450-455.
41. Lian H, Park D, Chen M, Schueder F, Lara-Tejero M, Liu J, Galán JE. 2023. Parkinson's disease kinase LRRK2 coordinates a cell-intrinsic itaconate-dependent defence pathway against intracellular Salmonella. Nat Microbiol 8:1880-1895.
42. Michelucci A, Cordes T, Ghelfi J, Pailot A, Reiling N, Goldmann O, Binz T, Wegner A, Tallam A, Rausell A, Buttini M, Linster CL, Medina E, Balling R, Hiller K. 2013. Immune-responsive gene 1 protein links metabolism to immunity by catalyzing itaconic acid production. Proc Natl Acad Sci U S A 110:7820-5.
43. Hiyoshi H, English BC, Diaz-Ochoa VE, Wangdi T, Zhang LF, Sakaguchi M, Haneda T, Tsolis RM, Bäumler AJ. 2022. Virulence factors perforate the pathogen-containing vacuole to signal efferocytosis. Cell Host Microbe 30:163-170.e6.
44. Knodler LA, Vallance BA, Celli J, Winfree S, Hansen B, Montero M, Steele-Mortimer O. 2010. Dissemination of invasive Salmonella via bacterial-induced extrusion of mucosal epithelia. Proc Natl Acad Sci U S A 107:17733-8.
45. Grant AJ, Morgan FJ, McKinley TJ, Foster GL, Maskell DJ, Mastroeni P. 2012. Attenuated Salmonella Typhimurium lacking the pathogenicity island-2 type 3 secretion system grow to high bacterial numbers inside phagocytes in mice. PLoS Pathog 8:e1003070.
46. Roudier C, Fierer J, Guiney DG. 1992. Characterization of translation termination mutations in the spv operon of the Salmonella virulence plasmid pSDL2. Journal of Bacteriology 174:6418-6423.
47. Guiney DG, Fierer J. 2011. The Role of the spv Genes in Salmonella Pathogenesis. Frontiers in Microbiology 2.
48. Lesnick ML, Reiner NE, Fierer J, Guiney DG. 2001. The Salmonella spvB virulence gene encodes an enzyme that ADP-ribosylates actin and destabilizes the cytoskeleton of eukaryotic cells. Mol Microbiol 39:1464-70.
49. Tezcan-Merdol D, Nyman T, Lindberg U, Haag F, Koch-Nolte F, Rhen M. 2001. Actin is ADP-ribosylated by the Salmonella enterica virulence-associated protein SpvB. Mol Microbiol 39:606-19.
50. Libby SJ, Lesnick M, Hasegawa P, Weidenhammer E, Guiney DG. 2000. The Salmonella virulence plasmid spv genes are required for cytopathology in human monocyte-derived macrophages. Cell Microbiol 2:49-58.
51. Mazurkiewicz P, Thomas J, Thompson JA, Liu M, Arbibe L, Sansonetti P, Holden DW. 2008. SpvC is a Salmonella effector with phosphothreonine lyase activity on host mitogen-activated protein kinases. Mol Microbiol 67:1371-83.

52. Haneda T, Ishii Y, Shimizu H, Ohshima K, Iida N, Danbara H, Okada N. 2012. Salmonella type III effector SpvC, a phosphothreonine lyase, contributes to reduction in inflammatory response during intestinal phase of infection. Cell Microbiol 14:485-99.
53. Zhu Y, Li H, Long C, Hu L, Xu H, Liu L, Chen S, Wang D-C, Shao F. 2007. Structural Insights into the Enzymatic Mechanism of the Pathogenic MAPK Phosphothreonine Lyase. Molecular Cell 28:899-913.
54. Grabe GJ, Zhang Y, Przydacz M, Rolhion N, Yang Y, Pruneda JN, Komander D, Holden DW, Hare SA. 2016. The Salmonella Effector SpvD Is a Cysteine Hydrolase with a Serovar-specific Polymorphism Influencing Catalytic Activity, Suppression of Immune Responses, and Bacterial Virulence. J Biol Chem 291:25853-25863.
55. Rolhion N, Furniss RCD, Grabe G, Ryan A, Liu M, Matthews SA, Holden DW. 2016. Inhibition of Nuclear Transport of NF-κB p65 by the Salmonella Type III Secretion System Effector SpvD. PLOS Pathogens 12:e1005653.
56. Hoiseth SK, Stocker BA. 1981. Aromatic-dependent Salmonella typhimurium are non-virulent and effective as live vaccines. Nature 291:238-9.
57. Datsenko KA, Wanner BL. 2000. One-step inactivation of chromosomal genes in Escherichia coli K-12 using PCR products. Proceedings of the National Academy of Sciences 97:6640-6645.
58. Deatherage DE, Barrick JE. 2014. Identification of mutations in laboratory-evolved microbes from next-generation sequencing data using breseq. Methods Mol Biol 1151:165-88.
59. Grant AJ, Restif O, McKinley TJ, Sheppard M, Maskell DJ, Mastroeni P. 2008. Modelling within-host spatiotemporal dynamics of invasive bacterial disease. PLoS Biol 6:e74.
60. Periaswamy B, Maier L, Vishwakarma V, Slack E, Kremer M, Andrews-Polymenis HL, McClelland M, Grant AJ, Suar M, Hardt WD. 2012. Live attenuated S. Typhimurium vaccine with improved safety in immuno-compromised mice. PLoS One 7:e45433.
61. Schubert C, Nguyen BD, Sichert A, Näpflin N, Sintsova A, Feer L, Näf J, Daniel BBJ, Steiger Y, von Mering C, Sauer U, Hardt W-D. 2024. Monosaccharides Drive Salmonella Gut Colonization in a Context-Dependent Manner. bioRxiv doi:10.1101/2024.08.06.606610:2024.08.06.606610.

Figure 1. Functional grouping of SPI-2 effector genes permits rationally designed multimutants

A) Graphic representation of reported functions for SPI-2 T3SS effector proteins. Effectors are loosely grouped into five different functional groups based on literature. Some effectors reportedly contribute to different functional groups and are represented twice here. **B)** Schematic representation of workflow to generate complex multimutants. Single mutants were created by lambda red recombination to replace genes of interest with cassettes encoding either kanamycin (::*aphT*) or chloramphenicol (::*cat*) resistance, followed by generation of P22 lysates containing phage that have packaged these deletions. Successive rounds of sequential P22 transduction and Flp-FRT removal of resistance cassettes resulted in mutants deficient for three to six effector genes, as required. Mutant strains were validated by whole genome sequencing to confirm deletion of target genes and to assess the degree of other changes to the genome. **C)** Rational design of SPI-2 effector multimutant strains based on reported functions described in **Fig 1A**. Six multimutant strains were constructed in duplicate and assigned designations based on the Greek alphabet (left) by deletion of effector genes in the sequence shown (right) to produce distinct multimutant genotypes (middle). **D)** Bioinformatic analysis confirming the deletion of target genes from corresponding multimutant strains. Blue rectangles correspond to absence of reads mapping to chromosomal regions encoding these genes. Two independently-constructed multimutant strains were analysed. Gene position (top) corresponds to position on the chromosome of S.Typhimurium SL1344, while other regions of the chromosome are not shown.

Figure 2. Systemic infection is compromised by deletion of SPI-2 effector cohorts

A) Experimental scheme to study virulence of S.Tm mutants during systemic infection *in vivo*. Mice were infected with 10^3 *S*.Tm by intraperitoneal injection. Mice were euthanised at day 4 post infection, and bacterial loads in the spleen and liver were quantified by CFU plating to selective media. **B)** S.Tm recovered from the liver (left) and spleen (right), (*n* = 5-7 mice per group). Horizontal bars denote median. Statistical differences between WT and indicated groups determined by two-tailed Mann Whitney-U test, ($p>0.05$ not significant (ns), $p<0.05$ (*), $p<0.01$ (**), $p<0.001$ (***). **C)** Experimental scheme to study relative fitness of S.Tm mutants *in vivo* by competitive infection. Mice were infected with a mixed inoculum comprising equal volumes of 9 different *S*.Tm strains each bearing unique chromosomal tags. Mice were euthanised at day 4 post infection. **D)** Relative proportion of each genetic tag determined by RT-qPCR. Data is presented as the proportion of a given tag relative to the other tags within one animal. Coloured circles represent tagged strain recovered from the liver (left) and spleen (right) of infected mice. Horizontal bars denote median.

Figure 3. SPI-2 effectors support bacterial migration to systemic niches

A)) Experimental scheme to study virulence of S.Tm mutants during oral infection *in vivo*. Mice were pre-treated with streptomycin by oral gavage, then received an infectious dose of 5x10^7 S.Tm by oral gavage. Faeces were collected at indicated time points and mice were euthanised at day 4 post infection. **B-C)** Bacterial loads recovered from **B)** the liver (left), spleen (right) and **C)** mesenteric lymph node at day 4 post infection (*n* = 5 mice per group). Dotted lines denote limit of detection. Horizontal bars denote median. **D)** Bacterial populations in the gut determined by CFU plating of homogenised faecal samples to selective media. Dotted line at 10^2 CFU / g faeces denotes conservative limit of detection (*n* = 5 mice per group). Horizontal bars denote median. **E-F)** Caecal histology at day 4 post infection. **E)** combined pathology score based on scoring criteria quantifying submucosal edema, epithelial barrier integrity, goblet cell number, and infiltration of polymorphonuclear granulocytes. **F)** representative micrographs of cecum samples stained with hematoxylin and eosin. Lu. lumen, S.E. submucosal edema. **B-C, E)** Statistical differences between WT and indicated groups determined by two-tailed Mann Whitney-U test, ($p>0.05$ not significant (ns), $p<0.05$ (*), $p<0.01$ (**), $p<0.001$ (***).

847 **Figure 4. Effector cohorts contribute to SPI-2 T3SS-dependent inflammation.**

848 **A)** Bacterial loads recovered from the liver (left), spleen (middle), and mesenteric lymph node
849 (right) at day 4 post infection (*n* = 5 mice per group). Mice were infected as in **Fig. 3A.** Dotted
850 lines denote limit of detection. Horizontal bars denote median. **B)** Bacterial populations in the
851 gut determined by CFU plating of homogenised faecal samples to selective media. Dotted line
852 at 10^2 CFU / g faeces denotes conservative limit of detection (*n* = 5 mice per group). Horizontal
853 bars denote median. **C)** Levels of gut inflammation at indicated days post infection determined
854 by ELISA quantification of lipocalin-2 (LCN2). Horizonal dotted line (upper) represents typical
855 threshold of moderately inflamed gut, while dotted line (lower) represents limit of detection.
856 Horizontal bars denote median. **D-E**) Caecal histology at day 4 post infection. **D)** combined
857 pathology score based on scoring criteria quantifying submucosal edema, epithelial barrier
858 integrity, goblet cell number, and infiltration of polymorphonuclear granulocytes. **E)**
859 representative micrographs of cecum samples stained with hematoxylin and eosin. Lu. lumen,
860 S.E. submucosal edema. **A, C-E)** Statistical differences between WT and indicated groups
861 determined by two-tailed Mann Whitney-U test, ($p>0.05$ not significant (ns), $p<0.05$ (*), $p<0.01$
862 (**), $p<0.001$ (***).

863

Figure 5. SPI-2 effectors SopD2 and GtgE contribute to SPI-2 T3SS-dependent inflammation

A-B) Bacterial loads in the liver (left), spleen (middle), and mesenteric lymph node (right) at day 4 post infection (*n* = 3-6 mice per group). Mice were infected as in **Fig 3A**. Dotted lines denote limit of detection. Horizontal bars denote median. **C)** Levels of gut inflammation at indicated days post infection determined by ELISA quantification of lipocalin-2 (LCN2). Horizonal dotted line (upper) represents typical threshold of moderately inflamed gut, while dotted line (lower) represents limit of detection. Horizontal bars denote median. **D)** Intracellular populations of bacteria recovered from cecal tissue by gentamicin protection assay. Dotted lines denote limit of detection. Horizontal bars denote median. **E-F)** Caecal histology at day 4 post infection. **E)** combined pathology score based on scoring criteria quantifying submucosal edema, epithelial barrier integrity, goblet cell number, and infiltration of polymorphonuclear granulocytes. **F)** representative micrographs of cecum samples stained with hematoxylin and eosin. Lu. lumen, S.E. submucosal edema. **A-C, E)** Statistical differences between WT and indicated groups determined by two-tailed Mann Whitney-U test, ($p>0.05$ not significant (ns), $p<0.05$ (*), $p<0.01$ (**), $p<0.001$ (***).

880 **Figure 6. Graphical summary effector cohort contributions to inflammation and systemic**
881 **colonisation.**

882 **A)** Genotypes of six SPI-2 T3SS effector multimutants generated by successive rounds of P22
883 transduction. Collectively, these strains cover all described SPI-2 effectors in the SL1344
884 background. **B)** Summary of phenotypic data described in **Fig 2-5**. S.Tm WT causes high levels of
885 gut inflammation and migrates from the gut to colonise systemic tissue, in a manner dependent
886 on the SPI-2 T3SS. Several multimutants show similar levels of virulence to WT. S.Tm Alpha,
887 Delta, and Zeta showed reduced colonisation of systemic niches, while SPI-2 T3SS-dependent
888 inflammation was impaired during infection with S.Tm Alpha and Delta. **C)** S.Tm WT relies on
889 intracellular niches to induce inflammation and achieve colonisation of systemic tissue. A
890 mutant deficient for SopD2 and GtgE fails to maintain the intracellular niche, leading to reduced
891 levels of gut inflammation and impaired colonisation of systemic sites.

892

893

Extended data Figure 1.

A) Bacterial loads recovered from the mesenteric lymph node (left) and faeces (right) at day 4 post infection, (*n* = 5-7 mice per group). Data pertains to **Fig 2B**. Dotted lines denote limit of detection. **B)** Bacterial loads recovered at day 2 post infection in the liver (upper left), spleen (upper right), mesenteric lymph node (bottom left), and faeces (bottom right). **A-B)** Statistical differences between WT and indicated groups determined by two-tailed Mann Whitney-U test, ($p>0.05$ not significant (ns), $p<0.05$ (*), $p<0.01$ (**), $p<0.001$ (***). **C)** Bacterial loads at indicated organs and in faeces at day 4 post infection. Data pertains to **Fig 2D. D)** Relative proportion of tagged strains recovered from the liver (upper) and spleen (lower) of individual animals, as denoted on the X axis. Horizontal bars denote median. Data pertains to **Fig 2D.**

Extended data Figure 2.

A-B) Bacterial populations in the gut determined by CFU plating of homogenised faecal samples to selective media. Dotted line at 10^2 CFU / g faeces denotes conservative limit of detection. **A)** Data pertains to **Fig. 5A**, (*n* = 3-6 mice per group). **B)** Data pertains to **Fig 5B**, (*n* = 5-7 mice per group).

910 **Table 1. Strains used in this study**

Strain name	Strain number	Relevant genotype	Resistance*	Reference
*S.*Tm SL1344	SB300	Wild-type	Sm	(56)
*S.*Tm Δ*invG*	SB161	Δ*invG*	Sm	(28)
*S.*Tm Δ*ssaV*	M2730	Δ*ssaV*	Sm	(60)
*S.*Tm Δ*invG*Δ*ssaV*	M2702	Δ*invG* Δ*ssaV*	Sm	(60)
*S.*Tm Efl	NA170	Δ*spvR* Δ*pipAB* Δ*pipB2* Δ*gtgA* Δ*sifB* Δ*gtgEsseI* Δ*steBsseJ* Δ*pipD* Δ*sseL* Δ*gogBsteE* Δ*sopD2* Δ*slrp* Δ*steA* Δ*steDsseK2* Δ*sspH2* Δ*sseK3* Δ*steC* Δ*cigR* Δ*sseK1* Δ*srfJ* Δ*sseFG* Δ*sifA*	Sm	(15)
S. Tm Alpha clone 1	T2978	Δ*sifA* Δ*sseJ* Δ*sseFG* Δ*pipB2* Δ*steA*	Sm	This study
S. Tm Alpha clone 2	T2979	Δ*sifA* Δ*sseJ* Δ*sseFG* Δ*pipB2* Δ*steA*	Sm	This study
S. Tm Beta clone 1	T2918	Δ*sseK1* Δ*sseK2* Δ*sseK3* Δ*gtgA* Δ*gogA* Δ*pipA*	Sm	This study
S. Tm Beta clone 2	T2919	Δ*sseK1* Δ*sseK2* Δ*sseK3* Δ*gtgA* Δ*gogA* Δ*pipA*	Sm	This study
S. Tm Gamma clone 1	T2974	Δ*steD* Δ*srgE* Δ*sseI* Δ*srfJ* Δ*steE* Δ*gogB*	Sm	This study
S. Tm Gamma clone 2	T2988	Δ*steD* Δ*srgE* Δ*sseI* Δ*srfJ* Δ*steE* Δ*gogB*	Sm	This study
S. Tm Delta clone 1	T2982	Δ*sopD2* Δ*gtgE* Δ*steC* Δ*sseL*	Sm	This study
S. Tm Delta clone 2	T2984	Δ*sopD2* Δ*gtgE* Δ*steC* Δ*sseL*	Sm	This study
S. Tm Epsilon clone 1	T2968	Δ*steB* Δ*cigR* Δ*sspH2* Δ*pipB* Δ*sifB* Δ*slrP*	Sm	This study
S. Tm Epsilon clone 2	T2966	Δ*steB* Δ*cigR* Δ*sspH2* Δ*pipB* Δ*sifB* Δ*slrP*	Sm	This study
S. Tm Zeta clone 1	T2860	Δ*spvR*	Sm	This study
S. Tm Zeta clone 2	T2861	Δ*spvR*	Sm	This study
*S.*Tm WT Tag 1	T3415	WISH 2	Sm, Amp	(61)
*S.*Tm Δ*ssaV* Tag 2	T2949	Δ*ssaV* WISH 7	Sm, Amp	This study
*S.*Tm *Efl* Tag 3	Z8294	Δ*spvR* Δ*pipAB* Δ*pipB2* Δ*gtgA* Δ*sifB* Δ*gtgEsseI* Δ*steBsseJ* Δ*pipD* Δ*sseL* Δ*gogBsteE* Δ*sopD2* Δ*slrp* Δ*steA* Δ*steDsseK2* Δ*sspH2* Δ*sseK3* Δ*steC* Δ*cigR* Δ*sseK1* Δ*srfJ* Δ*sseFG* Δ*sifA* WISH 3	Sm, Amp	This study
*S.*Tm Alpha Tag 4	T7400	Δ*sifA* Δ*sseJ* Δ*sseFG* Δ*pipB2* Δ*steA* WISH 5	Sm, Amp	This study

S.Tm Beta Tag 5	T2964	Δ*sseK1* Δ*sseK2* Δ*sseK3* Δ*gtgA* Δ*gogA* Δ*pipA* WISH 49	Sm, Amp	This study
S.Tm Gamma Tag 6	T7403	Δ*steD* Δ*srgE* Δ*sseI* Δ*srfJ* Δ*steE* Δ*gogB* WISH 19	Sm, Amp	This study
S.Tm Delta Tag 7	T7401	Δ*sopD2* Δ*gtgE* Δ*steC* Δ*sseL* WISH 10	Sm, Amp	This study
S.Tm Epsilon Tag 8	T7402	Δ*steB* Δ*cigR* Δ*sspH2* Δ*pipB* Δ*sifB* Δ*slrP* WISH 15	Sm, Amp	This study
S.Tm Zeta Tag 9	T2950	Δ*spvR* WISH 16	Sm, Amp	This study
S.Tm Alpha Δ*invG*	T2990	Δ*sifA* Δ*sseJ* Δ*sseFG* Δ*pipB2* Δ*steA* Δ*invG*	Sm	This study
S.Tm Beta Δ*invG*	T2954	Δ*sseK1* Δ*sseK2* Δ*sseK3* Δ*gtgA* Δ*gogA* Δ*pipA* Δ*invG*	Sm	This study
S. Tm Gamma Δ*invG*	T2992	Δ*steD* Δ*srgE* Δ*sseI* Δ*srfJ* Δ*steE* Δ*gogB* Δ*invG*	Sm	This study
S. Tm Delta Δ*invG*	T2994	Δ*sopD2* Δ*gtgE* Δ*steC* Δ*sseL* Δ*invG*	Sm	This study
S. Tm Epsilon Δ*invG*	T2996	Δ*steB* Δ*cigR* Δ*sspH2* Δ*pipB* Δ*sifB* Δ*slrP* Δ*invG*	Sm	This study
S.Tm Zeta Δ*invG*	T2998	Δ*spvR* Δ*invG*	Sm	This study
S.Tm Δ*steC* Δ*sseL*	Z8278	Δ*steC* Δ*sseL*	Sm	This study
S.Tm Δ*sopD2* Δ*gtgE*	T2816	Δ*sopD2::aphT* Δ*gtgE::cat*	Sm, Kan, Cm	This study
S.Tm Δ*sopD2::sopD2* Δ*gtgE::gtgE*	T2856	Δ*sopD2::sopD2* Δ*gtgE::gtgE*	Sm	This study
S.Tm Δ*sopD2* Δ*gtgE* Δ*invG*	T2824	Δ*sopD2::aphT* Δ*gtgE::cat* Δ*invG*	Sm, Kan, Cm	This study
S.Tm Alpha parent 1 clone 1	Z6643	Δ*sseF*Δ*sseG*::*aphT*	Sm, Kan	This study
S.Tm Alpha parent 1 clone 2	Z6644	Δ*sseF*Δ*sseG*::*aphT*	Sm, Kan	This study
S.Tm Alpha parent 2 clone 1	Z6655	Δ*sseF*Δ*sseG*::*aphT* Δ*sifA*::*cat*	Sm, Kan, Cm	This study
S.Tm Alpha parent 2 clone 2	Z6656	Δ*sseF*Δ*sseG*::*aphT* Δ*sifA*::*cat*	Sm, Kan, Cm	This study
S.Tm Alpha parent 3 clone 1	Z6681	Δ*sseF*Δ*sseG* Δ*sifA*	Sm	This study
S.Tm Alpha parent 3 clone 2	Z6682	Δ*sseF*Δ*sseG* Δ*sifA*	Sm	This study
S.Tm Alpha parent 4 clone 1	Z6693	Δ*sseF*Δ*sseG* Δ*sifA* Δ*sseJ*::*aphT*	Sm, Kan	This study
S.Tm Alpha parent 4 clone 2	Z6694	Δ*sseF*Δ*sseG* Δ*sifA* Δ*sseJ*::*aphT*	Sm, Kan	This study
S.Tm Alpha parent 5 clone 1	Z8161	Δ*sseF*Δ*sseG* Δ*sifA* Δ*sseJ::aphT* Δ*pipB2::cat*	Sm, Kan, Cm	This study
S.Tm Alpha parent 5 clone 2	Z8162	Δ*sseF*Δ*sseG* Δ*sifA* Δ*sseJ::aphT* Δ*pipB2::cat*	Sm, Kan, Cm	This study
S.Tm Alpha parent 6 clone 1	Z8199	Δ*sseF*Δ*sseG* Δ*sifA* Δ*sseJ* Δ*pipB2*	Sm	This study
S.Tm Alpha parent 6 clone 2	Z8200	Δ*sseF*Δ*sseG* Δ*sifA* Δ*sseJ* Δ*pipB2*	Sm	This study

S.Tm Alpha parent 7 clone 1	T2976	Δ*sseF*Δ*sseG* Δ*sifA* Δ*sseJ* Δ*pipB2 steA::aphT*	Sm, Kan	This study
S.Tm Alpha parent 7 clone 2	T2977	Δ*sseF*Δ*sseG* Δ*sifA* Δ*sseJ* Δ*pipB2 steA::aphT*	Sm, Kan	This study
S.Tm Beta parent 1 clone 1	Z5608	Δ*sseK2::cat*	Sm, Cm	This study
S.Tm Beta parent 1 clone 2	Z5600	Δ*sseK1::cat*	Sm, Cm	This study
S.Tm Beta parent 2 clone 1	Z5628	Δ*sseK2::cat* Δ*sseK3::aphT*	Sm, Kan, Cm	This study
S.Tm Beta parent 2 clone 2	Z5624	Δ*sseK1::cat* Δ*sseK2::aphT*	Sm, Kan, Cm	This study
S.Tm Beta parent 3 clone 1	Z5640	Δ*sseK2* Δ*sseK3*	Sm	This study
S.Tm Beta parent 3 clone 2	Z5636	Δ*sseK1* Δ*sseK2*	Sm	This study
S.Tm Beta parent 4 clone 1	Z5648	Δ*sseK2* Δ*sseK3* Δ*sseK1::aphT*	Sm, Kan	This study
S.Tm Beta parent 4 clone 2	Z5650	Δ*sseK1* Δ*sseK2* Δ*sseK3::aphT*	Sm, Kan	This study
S.Tm Beta parent 5 clone 1	Z5654	Δ*sseK2* Δ*sseK3* Δ*sseK1*	Sm	This study
S.Tm Beta parent 5 clone 2	Z5656	Δ*sseK1* Δ*sseK2* Δ*sseK3*	Sm	This study
S.Tm Beta parent 6 clone 1	T2900	Δ*sseK2* Δ*sseK3* Δ*sseK1* *gtgA::aphT*	Sm, Kan	This study
S.Tm Beta parent 6 clone 2	T2901	Δ*sseK1* Δ*sseK2* Δ*sseK3* *gtgA::aphT*	Sm, Kan	This study
S.Tm Beta parent 7 clone 1	T2904	Δ*sseK2* Δ*sseK3* Δ*sseK1* *gtgA::aphT gogA::cat*	Sm, Kan, Cm	This study
S.Tm Beta parent 7 clone 2	T2905	Δ*sseK1* Δ*sseK2* Δ*sseK3* *gtgA::aphT gogA::cat*	Sm, Kan, Cm	This study
S.Tm Beta parent 8 clone 1	T2914	Δ*sseK2* Δ*sseK3* Δ*sseK1* Δ*gtgA* Δ*gogA*	Sm	This study
S.Tm Beta parent 8 clone 2	T2915	Δ*sseK1* Δ*sseK2* Δ*sseK3* Δ*gtgA* Δ*gogA*	Sm	This study
S.Tm Beta parent 9 clone 1	T2916	Δ*sseK2* Δ*sseK3* Δ*sseK1* Δ*gtgA* Δ*gogA pipA::aphT*	Sm, Kan	This study
S.Tm Beta parent 9 clone 2	T2917	Δ*sseK1* Δ*sseK2* Δ*sseK3* Δ*gtgA* Δ*gogA pipA::aphT*	Sm, Kan	This study
S.Tm Gamma parent 1 clone 1	Z6539	Δ*steD::aphT*	Sm, Kan	This study
S.Tm Gamma parent 1 clone 2	Z6540	Δ*steD::aphT*	Sm, Kan	This study
S.Tm Gamma parent 2 clone 1	Z8117	Δ*steD::aphT* Δ*srgE::cat*	Sm, Kan, Cm	This study
S.Tm Gamma parent 2 clone 2	Z8118	Δ*steD::aphT* Δ*srgE::cat*	Sm, Kan, Cm	This study
S.Tm Gamma parent 3 clone 1	Z8193	Δ*steD* Δ*srgE*	Sm	This study
S.Tm Gamma parent 3 clone 2	Z8194	Δ*steD* Δ*srgE*	Sm	This study

S.Tm Gamma parent 4 clone 1	Z8211	*ΔsteD ΔsrgE ΔsseI::aphT*	Sm, Kan	This study
S.Tm Gamma parent 4 clone 2	Z8212	*ΔsteD ΔsrgE ΔsseI::aphT*	Sm, Kan	This study
S.Tm Gamma parent 5 clone 1	Z8215	*ΔsteD ΔsrgE ΔsseI::aphT ΔsrfJ::cat*	Sm, Kan, Cm	This study
S.Tm Gamma parent 5 clone 2	Z8216	*ΔsteD ΔsrgE ΔsseI::aphT ΔsrfJ::cat*	Sm, Kan, Cm	This study
S.Tm Gamma parent 6 clone 1	Z8221	*ΔsteD ΔsrgE ΔsseI ΔsrfJ*	Sm	This study
S.Tm Gamma parent 6 clone 2	Z8222	*ΔsteD ΔsrgE ΔsseI ΔsrfJ*	Sm	This study
S.Tm Gamma parent 7 clone 1	Z8227	*ΔsteD ΔsrgE ΔsseI ΔsrfJ ΔsteE::aphT*	Sm, Kan	This study
S.Tm Gamma parent 7 clone 2	Z8228	*ΔsteD ΔsrgE ΔsseI ΔsrfJ ΔsteE::aphT*	Sm, Kan	This study
S.Tm Gamma parent 8 clone 1	T2902	*ΔsteD ΔsrgE ΔsseI ΔsrfJ ΔsteE*	Sm	This study
S.Tm Gamma parent 8 clone 2	T2903	*ΔsteD ΔsrgE ΔsseI ΔsrfJ ΔsteE*	Sm	This study
S.Tm Gamma parent 9 clone 1	T2972	*ΔsteD ΔsrgE ΔsseI ΔsrfJ ΔsteE gogB::aphT*	Sm, Kan	This study
S.Tm Gamma parent 9 clone 2	T2986	*ΔsteD ΔsrgE ΔsseI ΔsrfJ ΔsteE gogB::aphT*	Sm, Kan	This study
S.Tm Delta parent 1 clone 1	Z6535	*ΔsteC::aphT*	Sm, Kan	This study
S.Tm Delta parent 1 clone 2	Z6536	*ΔsteC::aphT*	Sm, Kan	This study
S.Tm Delta parent 2 clone 1	Z8270	*ΔsteC::aphT ΔsseL::cat*	Sm, Kan, Cm	This study
S.Tm Delta parent 2 clone 2	Z8271	*ΔsteC::aphT ΔsseL::cat*	Sm, Kan, Cm	This study
S.Tm Delta parent 3 clone 1	Z8278	*ΔsteC ΔsseL*	Sm	This study
S.Tm Delta parent 3 clone 2	Z8279	*ΔsteC ΔsseL*	Sm	This study
S.Tm Delta parent 4 clone 1	Z8286	*ΔsteC ΔsseL sopD2::aphT*	Sm, Kan	This study
S.Tm Delta parent 4 clone 2	Z8289	*ΔsteC ΔsseL sopD2::aphT*	Sm, Kan	This study
S.Tm Delta parent 5 clone 1	T2804	*ΔsteC ΔsseL sopD2::aphT gtgE::cat*	Sm, Kan, Cm	This study
S.Tm Delta parent 5 clone 2	T2805	*ΔsteC ΔsseL sopD2::aphT gtgE::cat*	Sm, Kan, Cm	This study
S.Tm Epsilon parent 1 clone 1	Z6525	*ΔsteB::cat*	Sm, Kan	This study
S.Tm Epsilon parent 1 clone 2	Z6526	*ΔsteB::cat*	Sm, Kan	This study
S.Tm Epsilon parent 2 clone 1	Z8115	*ΔsteB::cat ΔcigR::aphT*	Sm, Kan, Cm	This study
S.Tm Epsilon parent 2 clone 2	Z8116	*ΔsteB::cat ΔcigR::aphT*	Sm, Kan, Cm	This study

S.Tm Epsilon parent 3 clone 1	Z8191	*ΔsteB ΔcigR*	Sm	This study
S.Tm Epsilon parent 3 clone 2	Z8192	*ΔsteB ΔcigR*	Sm	This study
S.Tm Epsilon parent 4 clone 1	Z8209	*ΔsteB ΔcigR ΔsspH2::aphT*	Sm, Kan	This study
S.Tm Epsilon parent 4 clone 2	Z8210	*ΔsteB ΔcigR ΔsspH2::aphT*	Sm, Kan	This study
S.Tm Epsilon parent 5 clone 1	Z8219	*ΔsteB ΔcigR ΔsspH2::aphT pipB::cat*	Sm, Kan, Cm	This study
S.Tm Epsilon parent 5 clone 2	Z8220	*ΔsteB ΔcigR ΔsspH2::aphT pipB::cat*	Sm, Kan, Cm	This study
S.Tm Epsilon parent 6 clone 1	Z8223	*ΔsteB ΔcigR ΔsspH2 ΔpipB*	Sm	This study
S.Tm Epsilon parent 6 clone 2	Z8224	*ΔsteB ΔcigR ΔsspH2 ΔpipB*	Sm	This study
S.Tm Epsilon parent 7 clone 1	T2924	*ΔsteB ΔcigR ΔsspH2 ΔpipB slrP::aphT*	Sm, Kan	This study
S.Tm Epsilon parent 7 clone 2	T2925	*ΔsteB ΔcigR ΔsspH2 ΔpipB slrP::aphT*	Sm, Kan	This study
S.Tm Epsilon parent 8 clone 1	T2935	*ΔsteB ΔcigR ΔsspH2 ΔpipB slrP::aphT sifB::cat*	Sm, Kan, Cm	This study
S.Tm Epsilon parent 8 clone 2	T2936	*ΔsteB ΔcigR ΔsspH2 ΔpipB slrP::aphT sifB::cat*	Sm, Kan, Cm	This study
S.Tm Zeta parent 1 clone 1	Z8264	*ΔspvR::aphT*	Sm, Kan	This study
S.Tm Zeta parent 1 clone 2	Z8265	*ΔspvR::aphT*	Sm, Kan	This study

***Resistances:** Sm = 50 µg/ml streptomycin, Amp = 50 µg/ml ampicillin, Cm = 15 µg/ml chloramphenicol, Kan = 50 µg/ml kanamycin.

914 **Table 2. Primers used in this study**

Primer name	Sequence	Source	Purpose
slrP_FW	GACGACTGTGACCTCTTATTTAAA	This study	Genotyping of slrP deletion
slrP_RV	AAAAAGCGCTACAGGCGTTGG	This study	Genotyping of slrP deletion
sopD2_FW	TTTCTAAACCCAGGCTGATTCAA	This study	Genotyping of sopD2 deletion
sopD2_RV	CCATGTAATGGGTTTGACTGAAA	This study	Genotyping of sopD2 deletion
gtgA_FW	TAGGCAATGAGTCCGGCCA	This study	Genotyping of gtgA deletion
gtgA_RV	CCTTGGCAGGGCTCGCT	This study	Genotyping of gtgA deletion
sseI_FW	TATTGTGAAATTAAGACCAGGAAGA	This study	Genotyping of sseI deletion
sseI_RV	GATGTTGTTGTCGATCTCCAC	This study	Genotyping of sseI deletion
gtgE_FW	ATGCGACAATACAATAAAAACATATCA	This study	Genotyping of gtgE deletion
gtgE_RV	AGCTTCCCCGTAGGAAATTGA	This study	Genotyping of gtgE deletion
pipA_FW	GTTGGCTTTGTCTGAATCATAGC	This study	Genotyping of pipA deletion
pipA_RV	GCCCCTTTGTTTTTTTAGGCG	This study	Genotyping of pipA deletion
pipB_FW	CAAAGCTCTAAATACAAAAATCACC	This study	Genotyping of pipB deletion
pipB_RV	TGAAACTTAGGGGCGGGGTT	This study	Genotyping of pipB deletion
sifA_FW	GCGCCCGCAGTTGAGATAAA	This study	Genotyping of sifA deletion
sifA_RV	GCCTGGCAAGAGGTTACTCA	This study	Genotyping of sifA deletion
sseF_FW	CGGATGCCTCATGGAGTGA	This study	Genotyping of sseF deletion
sseG_RV	CATCGTAAGGATACTGGCAACA	This study	Genotyping of sseG deletion
srgE_FW	ATGAGTTATTGACCACTGAATTTTCT	This study	Genotyping of srgE deletion
srgE_RV	GAGTAACTTTACGACAATTGCTTC	This study	Genotyping of srgE deletion
steA_FW	CTGAAAATGTATGCCTTTGAGCAA	This study	Genotyping of steA deletion
steA_RV	TTCTGAGAATCTCTTTGCGACAC	This study	Genotyping of steA deletion
sifB_FW	AAAGCAAAAATCAGGTGTTTCACC	This study	Genotyping of sifB deletion
sifB_RV	TTCGTTCCATAGTAAATCCATTATTC	This study	Genotyping of sifB deletion
steB_FW	CTTAGTCAATGTGGACAAAAAATCAAA	This study	Genotyping of steB deletion
steB_RV	ACGGCAGAACTTCCCATAGC	This study	Genotyping of steB deletion
sseJ_FW	AAGAAGCGTAATTCCATATACACC	This study	Genotyping of sseJ deletion
sseJ_RV	CAATCGGCAGCAAAGATAGCAT	This study	Genotyping of sseJ deletion

steC_FW	CAAACTGGCAAATCAAAGAGTCT	This study	Genotyping of steC deletion
steC_RV	TTGCATCTCCGCTACAGGCT	This study	Genotyping of steC deletion
sseK3_FW	TTAAGCCCCCCCTAACCAAGTAAAAACTATCGTTTCAGAT	This study	Genotyping of sseK3 deletion
sseK3_RV	TTCACCACGGCACGCAGGTCATCCAATTTAATGGAGGTAC	This study	Genotyping of sseK3 deletion
sseK2_FW	GTCGGACTCAGGACTTAGCATTGTGACGTTAACGTTTAAA	This study	Genotyping of sseK2 deletion
sseK2_RV	TGAAAGTTCTGTAGAGAAACTTGAATGTGAAATTGAGGTA	This study	Genotyping of sseK2 deletion
steD_FW	CCTATTTAGATGATGGCTTAGCG	This study	Genotyping of steD deletion
steD_RV	CTATATAAGTCATAAGCCTCTGGT	This study	Genotyping of steD deletion
sspH2_FW	TCTGCACCTTCTGAAGCCC	This study	Genotyping of sspH2 deletion
sspH2_RV	GTCATCCGGATATTTCACCTGT	This study	Genotyping of sspH2 deletion
sseL_FW	GCAATATCTCTTGTATCGACGC	This study	Genotyping of sseL deletion
sseL_RV	GACAGCAGGTTGGCGATGT	This study	Genotyping of sseL deletion
gogB_FW	TAGGTTCTAAATCTTGCCTGAATG	This study	Genotyping of gogB deletion
gogB_RV	AAGTTGGCATGTAGTCTAGAGTTA	This study	Genotyping of gogB deletion
steE_FW	TCTTGTTGTGATGAGATTCGTATATA	This study	Genotyping of steE deletion
steE_RV	AAATCACACAATCCGGACTGAG	This study	Genotyping of steE deletion
gogA_FW	GCTTTTAGCTTAATTGATTGCGTG	This study	Genotyping of gogA deletion
gogA_RV	ATTCCATTTGAGGCTGCCATTC	This study	Genotyping of gogA deletion
pipB2_FW	TTATTATGTAACCAGACGTAAAGGG	This study	Genotyping of pipB2 deletion
pipB2_RV	TTTTACCGTCGCATACTCCTGT	This study	Genotyping of pipB2 deletion
cigR_FW	ATAAGCTGCTGTTGGCGAGC	This study	Genotyping of cigR deletion
cigR_RV	CGTAGCGAGTCAAACCTCAC	This study	Genotyping of cigR deletion
sseK1_FW	CTGGCAGGGTATTTATGTATCCTCCGGTTAATGCTTAGTT	This study	Genotyping of sseK1 deletion
sseK1_RV	AATGCCGTATATCTCCGTTCTGAACAGCACTGCGATTTTA	This study	Genotyping of sseK1 deletion
srfJ_FW	GACTGGAAACAGCGCTTTATTGATGCC	This study	Genotyping of srfJ deletion
srfJ_RV	GTCGCTTCATTAAATCCCAGCT	This study	Genotyping of srfJ deletion
spvR_FW	CATAATCCTATCCAGTAACCCC	This study	Genotyping of spvB deletion
spvR_RV	GGTGAACTACCGCTATGGAG	This study	Genotyping of spvB deletion
pipB_red_FW	CCTATAAGGAGTCGGCTCACTTCCATAAGAAGGAATCAAAATATGAATATCCTCCTTAGTTCC	This study	Lambda red replacement of pipB

pipB_red_RV	TGTTTGAATACTTCTTGTTTATAAAATCCCTTTATCTC GATGTGTAGGCTGGAGCTGCTTC	This study	Lambda red replacement of pipB
srgE_red_FW	ACTACACTGGGAAATCGTTGCGTGGTGGTTCCGGAGAT AGATATGAATATCCTCCTTAGTTCC	This study	Lambda red replacement of srgE
srgE_red_RV	AATGCCAGACTTCCGCTACCAGACGGTATACACAGTAT TATGTGTAGGCTGGAGCTGCTTC	This study	Lambda red replacement of srgE
sseJ_red_FW	TTATTTGCTAAAGCGTGTTTAATAAAGTAAGGAGGACA CTATATGAATATCCTCCTTAGTTCC	This study	Lambda red replacement of sseJ
sseJ_red_RV	AGCTGTGTTTTGCTCAAGGCGTACCGCAGCCGATGGAA CTTGTGTAGGCTGGAGCTGCTTC	This study	Lambda red replacement of sseJ
gtgA_red_FW	AATGTTAATTCCATGTAATAAAAAGGATGTGTAACTCA TCATATGAATATCCTCCTTAGTTCC	This study	Lambda red replacement of gtgA
gtgA_red_RV	GTGTTGTAGCATCGTGGGATTTTGCATTTTTTGATGAG TGTGTGTAGGCTGGAGCTGCTTC	This study	Lambda red replacement of gtgA
gtgE_red_FW	TATAATTACATTAACAAAATTACTATTCGGCGAGTATA TTATATGAATATCCTCCTTAGTTCC	This study	Lambda red replacement of gtgE
gtgE_red_RV	AATTATCTTGGTAAAGGTTAACTATCATAAAATGGTAC ACTGTGTAGGCTGGAGCTGCTTC	This study	Lambda red replacement of gtgE
sseL_red_FW	ATTGAGCATACCGCAATTTCACAGCTTATATACAGAAG AGATATGAATATCCTCCTTAGTTCC	This study	Lambda red replacement of sseL
sseL_red_RV	AGGATAAGAGCCTAATGGGATAGGCTCTAAGTACTCAC CATGTGTAGGCTGGAGCTGCTTC	This study	Lambda red replacement of sseL
gogB_red_FW	ATTGAAAAAGCGCATGAAAATAGGATTCCAACCAGCCA TAATATGAATATCCTCCTTAGTTCC	This study	Lambda red replacement of gogB
gogB_red_RV	GCTCTATATATAAATATATTAATTGCATATTTTTTTAA AGTGTGTAGGCTGGAGCTGCTTC	This study	Lambda red replacement of gogB
gogA_red_FW	AATGTTAATTCCATGTAATAAAAAGGATGTGTAACTCA TCATATGAATATCCTCCTTAGTTCC	This study	Lambda red replacement of gogA
gogA_red_RV	GTGTTGTAGCATCGTGGGATTTTGCATTTTTTGATGAG TGTGTGTAGGCTGGAGCTGCTTC	This study	Lambda red replacement of gogA
sseFsseG_red_FW	AATGGTTGATACTCTTATTGCTTAAATAACAGAACGAA ATATATGAATATCCTCCTTAGTTCC	This study	Lambda red replacement of sseFsseG
sseFsseG_red_RV	TTTAGAAAGCAATGAACATCCGGTATATACCTGAAAAC GATGTGTAGGCTGGAGCTGCTTC	This study	Lambda red replacement of sseFsseG
sspH2_red_FW	CGGACAGATACTATATGTAAATTTATAAAGGTTTTTTG TTATATGAATATCCTCCTTAGTTCC	This study	Lambda red replacement of sspH2
sspH2_red_RV	GGAATATCTTTGTCGCACCGCACCTCATTCACCTGGTG CATGTGTAGGCTGGAGCTGCTTC	This study	Lambda red replacement of sspH2
sopD2_red_FW	TTGGATCTTGCTTTCGCGGTAAATAATCAAGGGAGTTA TTATATGAATATCCTCCTTAGTTCC	This study	Lambda red replacement of sopD2

sopD2_red_RV	AAAAAAGGCTCCATATCAGTGGGGCCTTTTTAATGACTTTTGTGTAGGCTGGAGCTGCTTC	This study	Lambda red replacement of sopD2
steA_red_FW	GACATATAAAGCTATTGAGCAAAATTTGAAGGAGTAGGATATATGAATATCCTCCTTAGTTCC	This study	Lambda red replacement of steA
steA_red_RV	AGTCTGATTTCTAACAAAACTGGCTAAACATAAACGCTTTTGTGTAGGCTGGAGCTGCTTC	This study	Lambda red replacement of steA
steB_red_FW	TCATTATTGTTAGTTTGAAATCAATCTCAGGTAATAATCCATATGAATATCCTCCTTAGTTCC	This study	Lambda red replacement of steB
steB_red_RV	CTGTGGAATAGCAATGCCGGGAAGGACATGGCATGACACTTGTGTAGGCTGGAGCTGCTTC	This study	Lambda red replacement of steB
steC_red_FW	TTGCATGTGTATTATAATAAATTTTCAGAGGATGAGACATATATGAATATCCTCCTTAGTTCC	This study	Lambda red replacement of steC
steC_red_RV	TGTGCCCCCGGCGATTCGCAGAAAAGAACGGAACTAAATGTGTGTAGGCTGGAGCTGCTTC	This study	Lambda red replacement of steC
sifB_red_FW	CCAGTAATGAAGTATCATATAATCACTTGTGGTCTACATTATATGAATATCCTCCTTAGTTCC	This study	Lambda red replacement of sifB
sifB_red_RV	ATTGCCAGGGGATTGTAAATCCATACTATTTATGGTGTGATGTGTAGGCTGGAGCTGCTTC	This study	Lambda red replacement of sifB
slrP_red_FW	TCTGTTACTTTAGGTTACGTTCAGATCAGGTAGGGAAAATATATGAATATCCTCCTTAGTTCC	This study	Lambda red replacement of slrP
slrP_red_RV	GTAAACAGGCTCTCTCCCTCTTCTGATAAACTGCGTTCAGATATGAATATCCTCCTTAGTTCC	This study	Lambda red replacement of slrP
BamHI_sopD2_FW	ATTTGGATCCACAGGCGCGAAACCAGTC	This study	Complementation insert for sopD2 with restriction sites
NotI_sopD2_RV	ATTTGCGGCCGCATCAAAGGCGATGTTCTGAACTT	This study	Complementation insert for sopD2 with restriction sites
BamHI_gtgE_FW	ATTTGGATCCTTCGGCATCGAGGTCAAAGG	This study	Complementation insert for gtgE with restriction sites
NotI_gtgE_RV	ATTTGCGGCCGCGGGACAGTCATCCGTTTTTAAC	This study	Complementation insert for gtgE with restriction sites

915

A

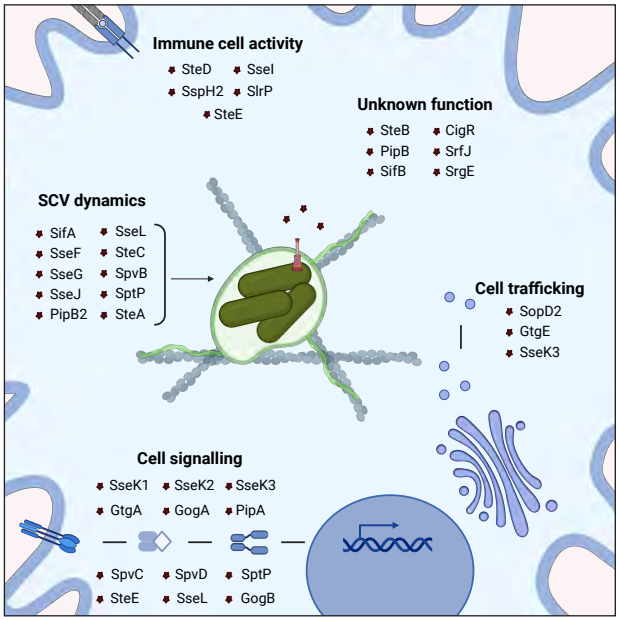

B

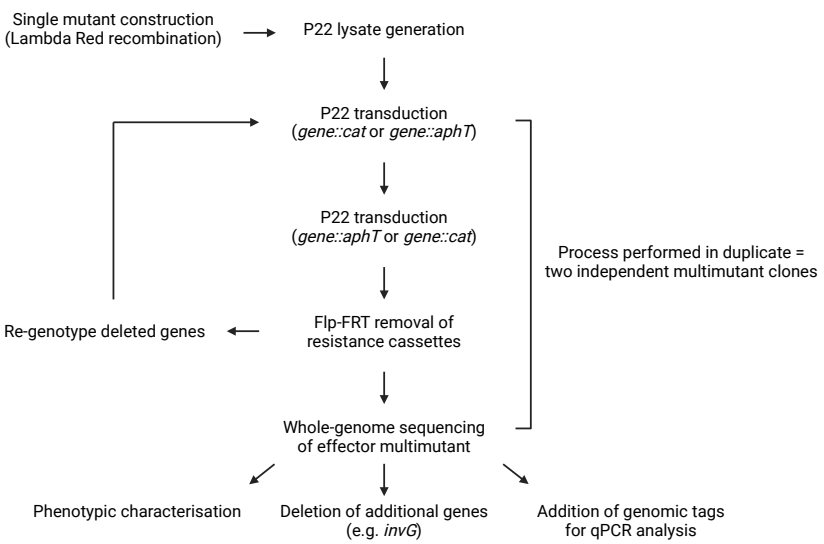

C

Strain	Genotype	Deletion sequence					
		1st →	2nd →	3rd →	4th →	5th →	6th
*S.*Tm Alpha	Δ*sseF*Δ*sseG* Δ*sifA* Δ*sseJ* Δ*pipB2* Δ*steA*	Δ*sseF*Δ*sseG*	Δ*sifA*	Δ*sseJ*	Δ*pipB2*	Δ*steA*	
*S.*Tm Beta	Δ*sseK2* Δ*sseK3* Δ*sseK1* Δ*gtgA* Δ*gogA* Δ*pipA*	Δ*sseK2*	Δ*sseK3*	Δ*sseK1*	Δ*gtgA*	Δ*gogA*	Δ*pipA*
*S.*Tm Gamma	Δ*steD* Δ*srgE* Δ*sseI* Δ*srfJ* Δ*steE* Δ*gogB*	Δ*steD*	Δ*srgE*	Δ*sseI*	Δ*srfJ*	Δ*steE*	Δ*gogB*
*S.*Tm Delta	Δ*steC* Δ*sseL* Δ*sopD2* Δ*gtgE*	Δ*steC*	Δ*sseL*	Δ*sopD2*	Δ*gtgE*		
*S.*Tm Epsilon	Δ*steB* Δ*cigR* Δ*sspH2* Δ*pipB* Δ*slrP* Δ*sifB*	Δ*steB*	Δ*cigR*	Δ*sspH2*	Δ*pipB*	Δ*slrP*	Δ*sifB*
*S.*Tm Zeta	Δ*spvR*	Δ*spvR*					

D

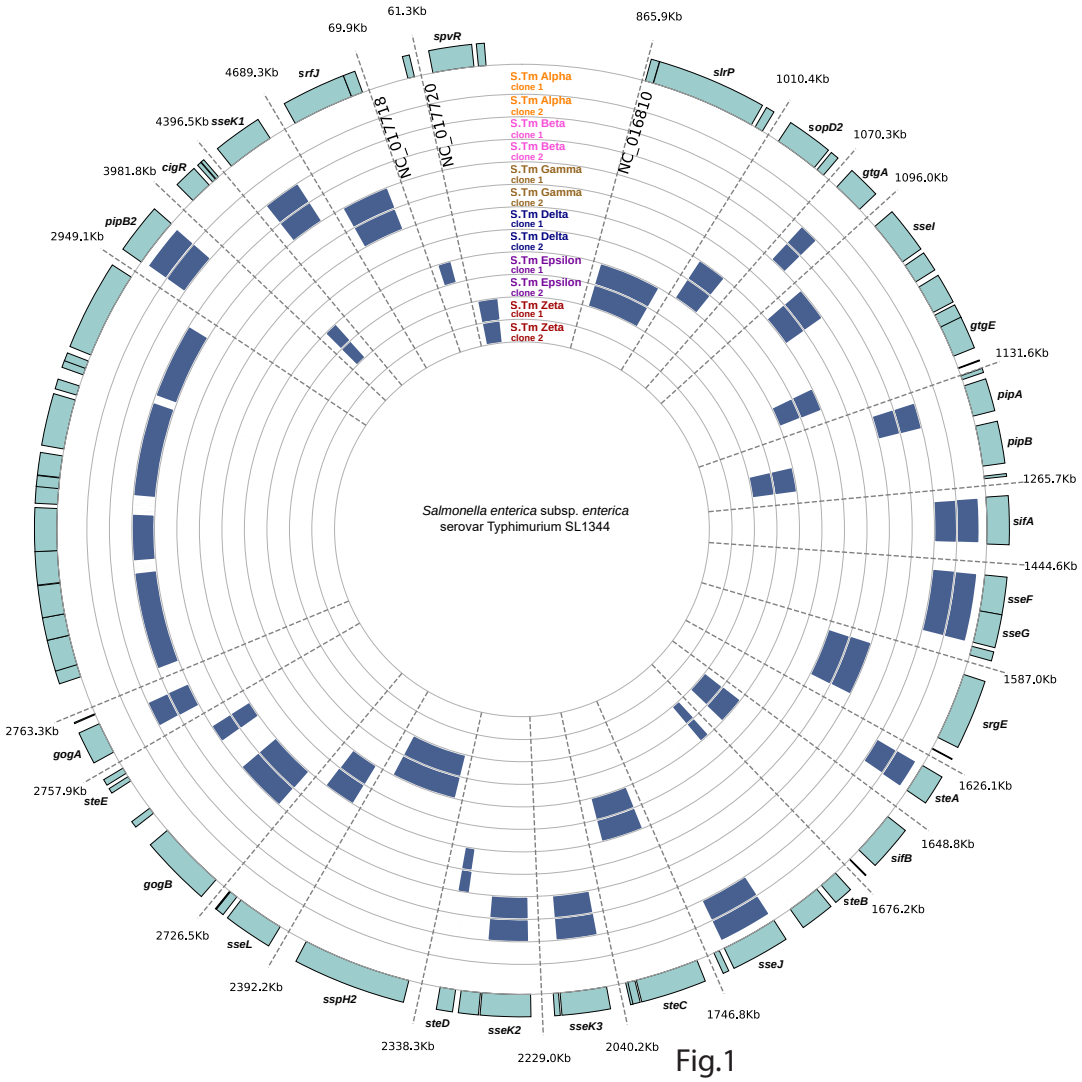

Fig.1

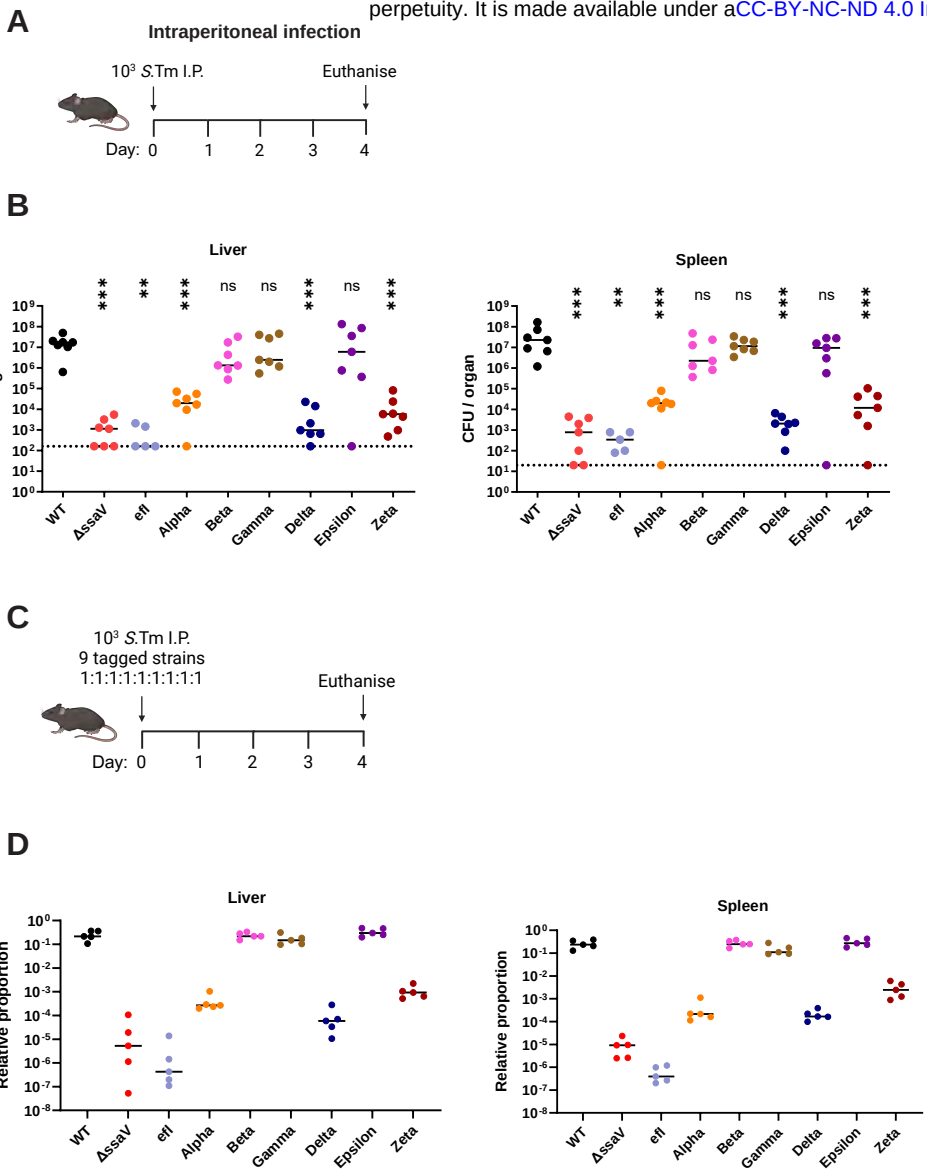

Fig.2

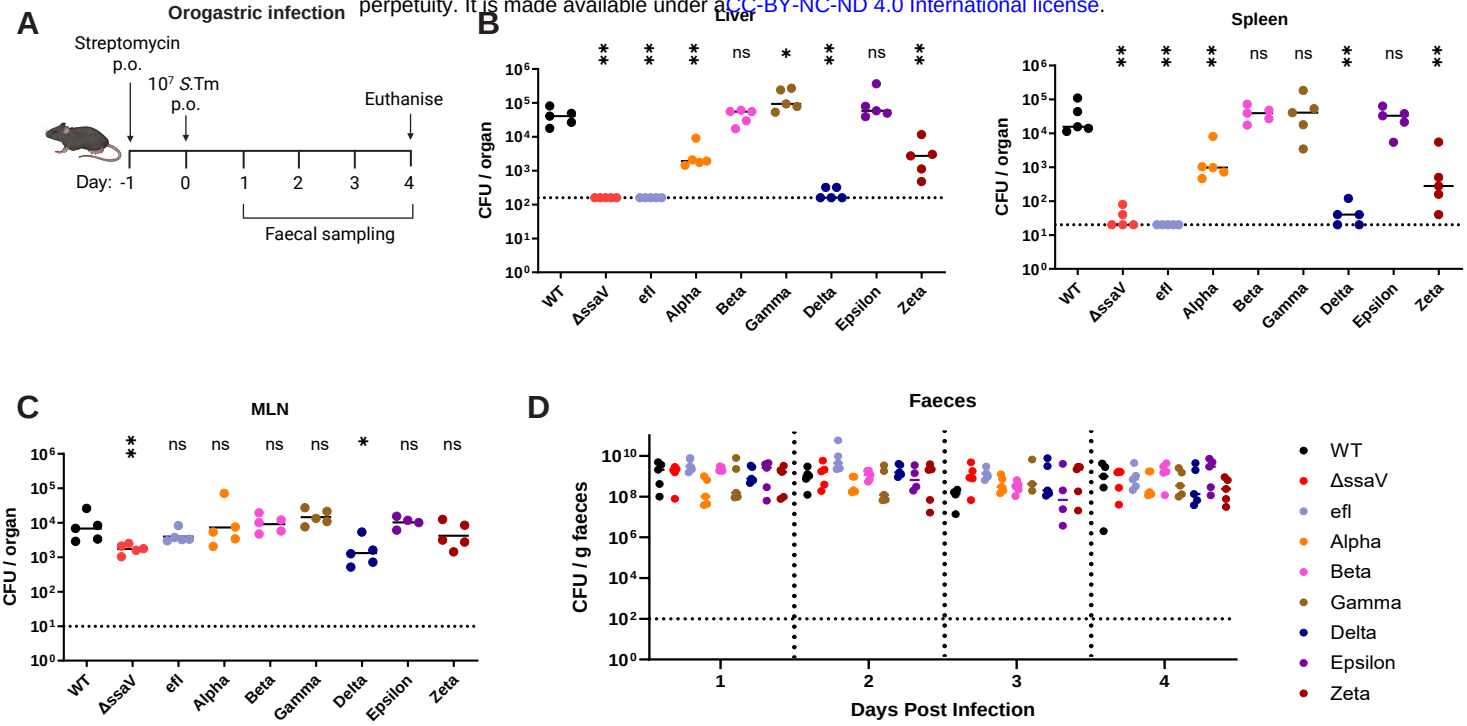

Fig.3

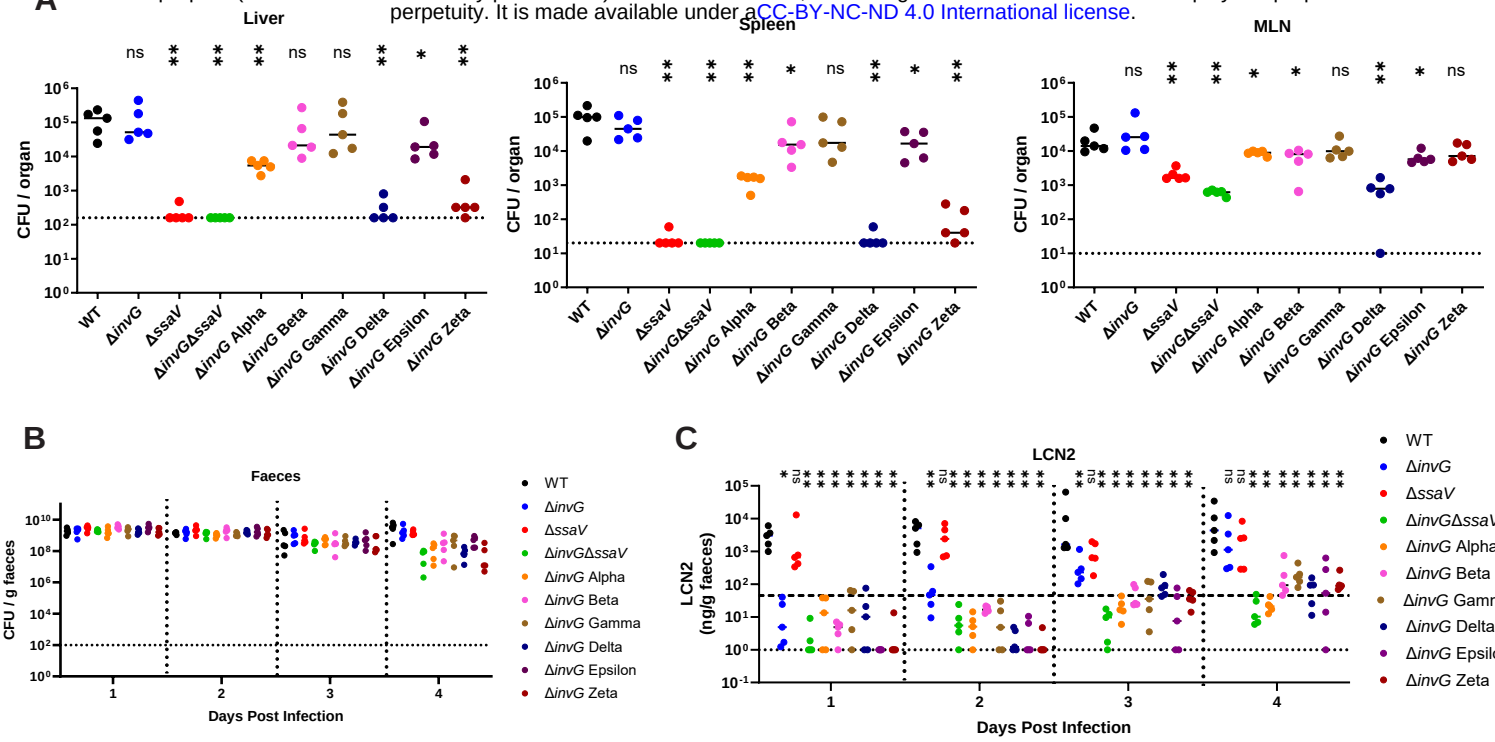

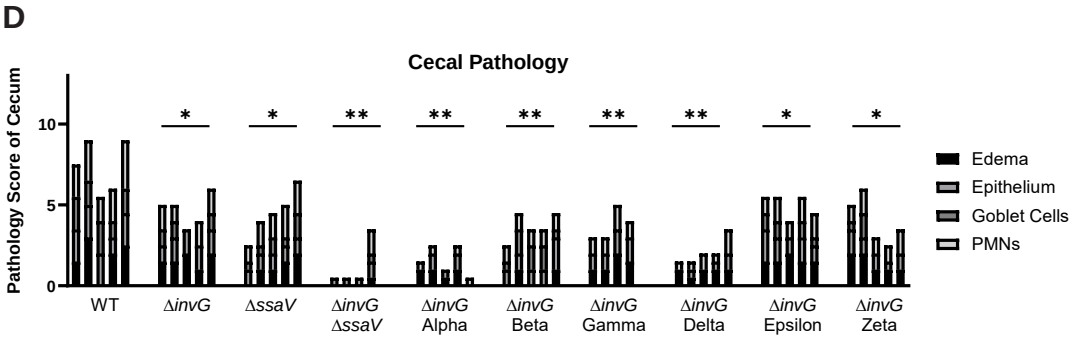

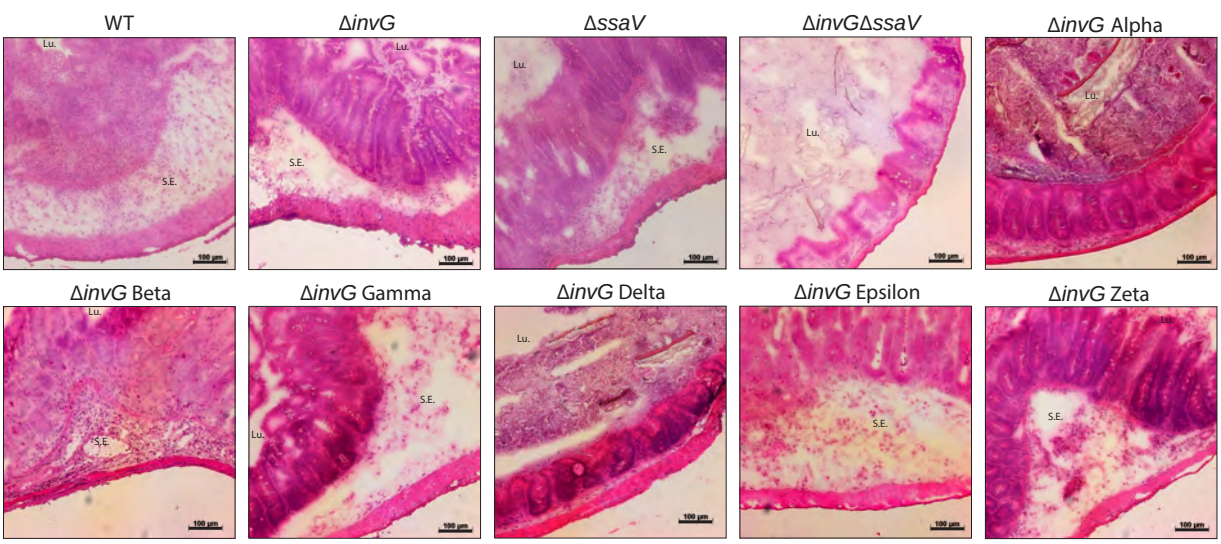

Fig.4

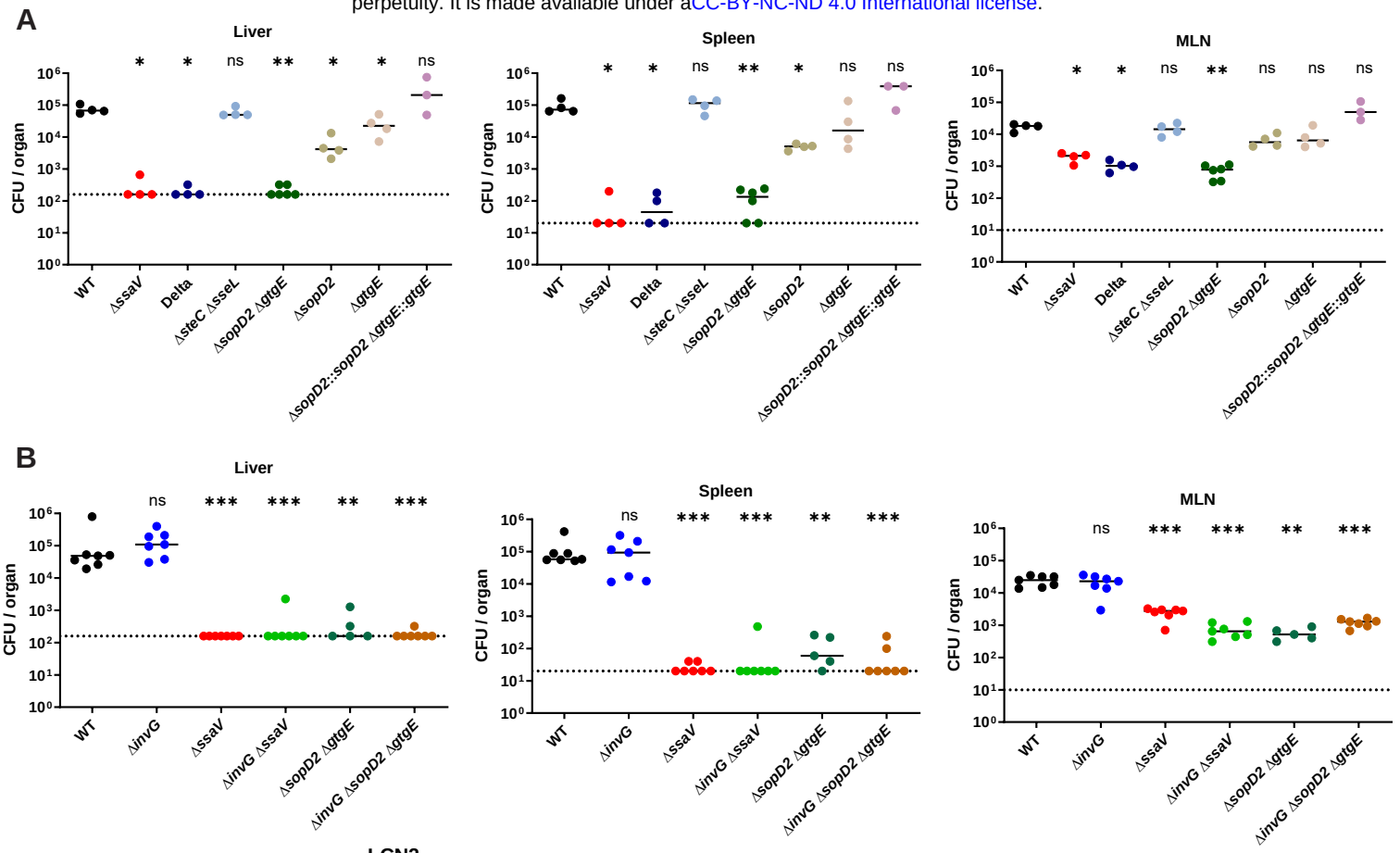

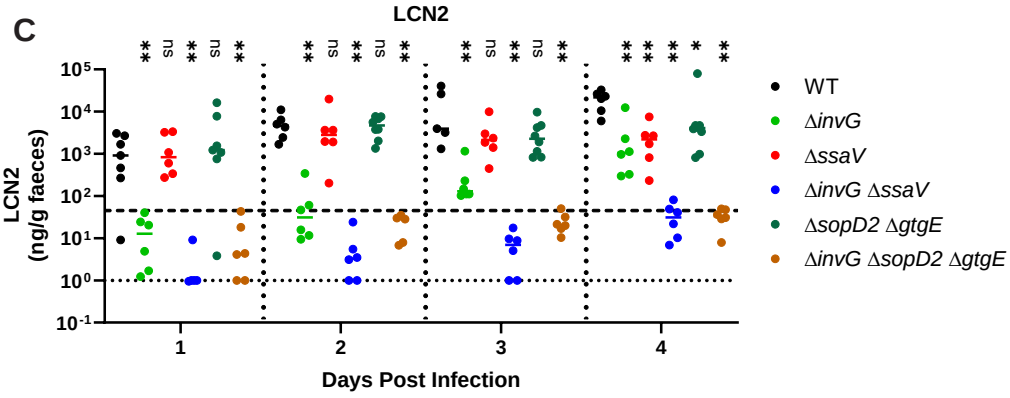

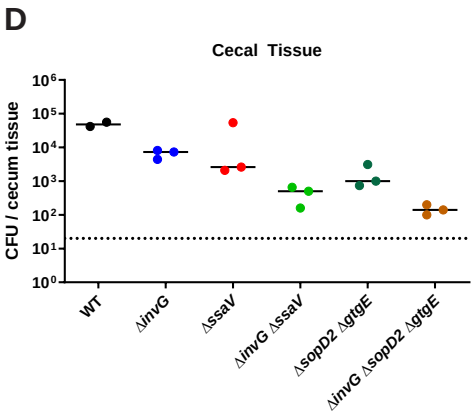

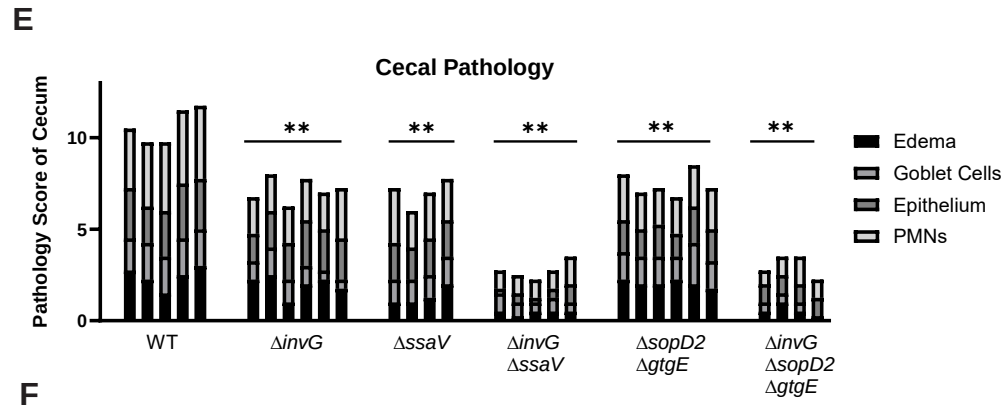

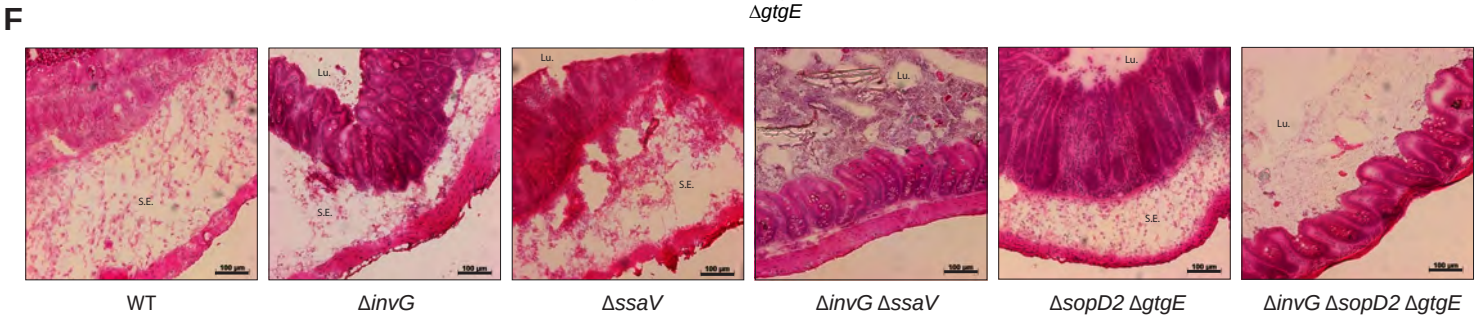

Fig.5

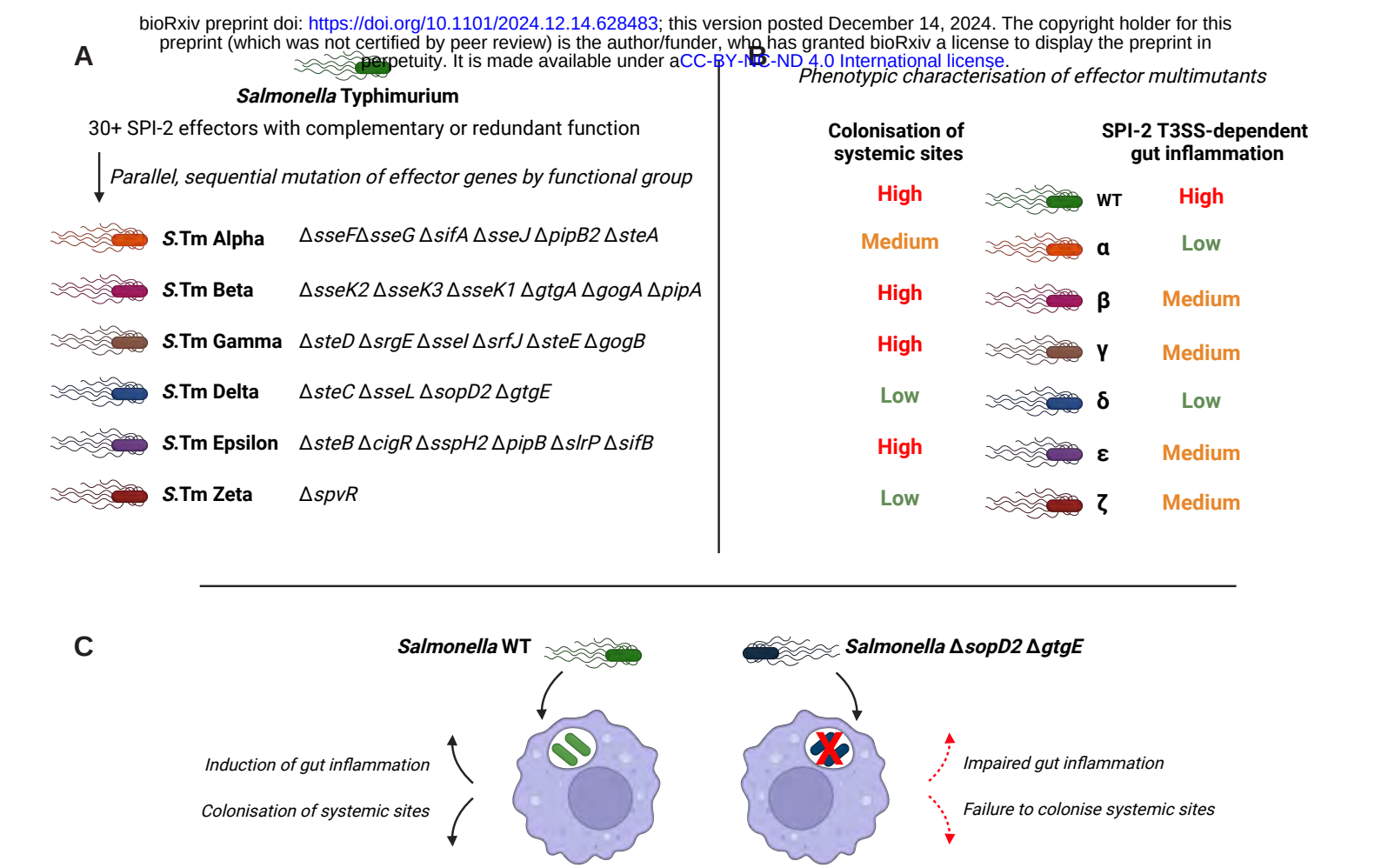

Fig.6

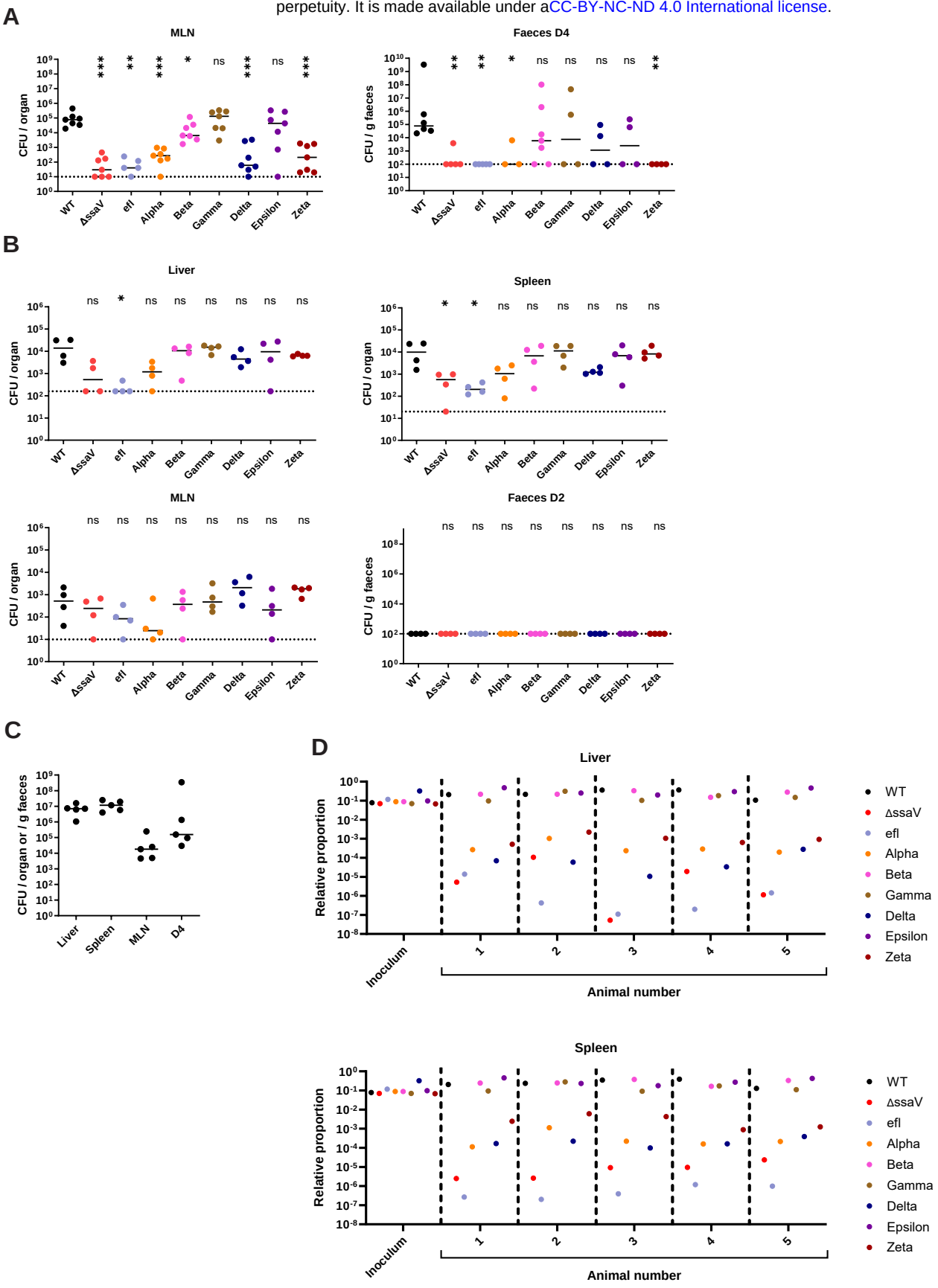

Fig.S1

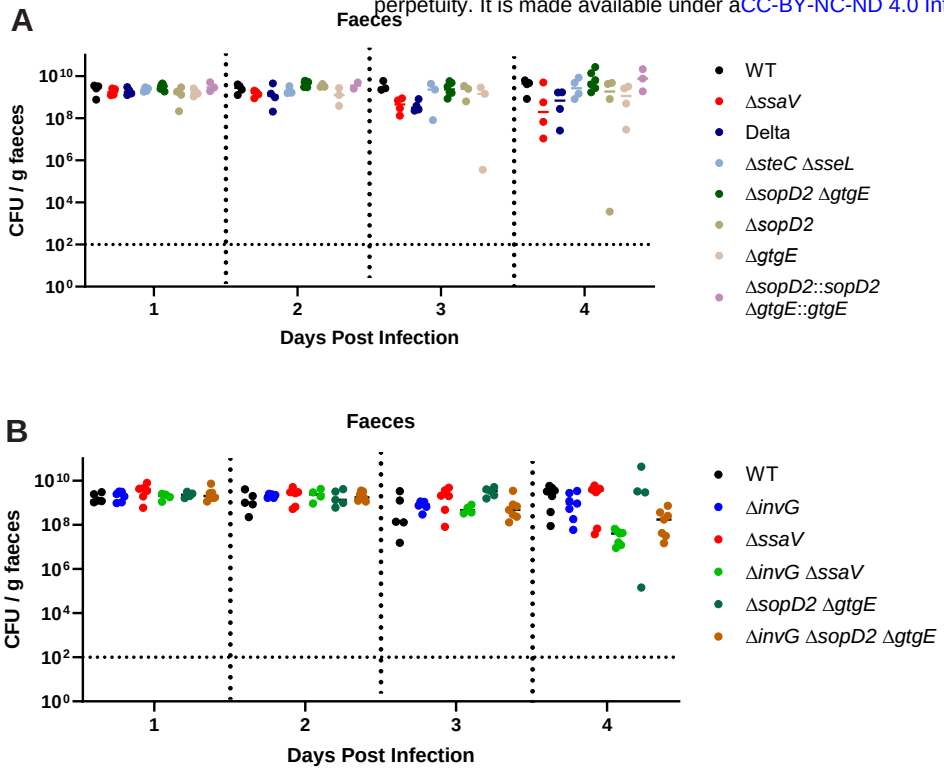

Fig.S2

Table S1 - List of polymorphisms detected via whole genome sequencing

strain	origin	evidence	chr	pos	mutation	annotation	gene	description
S.Tm Alpha clone 1	STm14028	RA	NC_016810	635606	T→A	E95V(GAG→GTG)	SL1344_RS02910←	PTS system mannose/fructose/N-acetylgalactosamine-transporter subunit IIB
S.Tm Alpha clone 1	STm14028	RA	NC_016810	1638110	A→G	T55A(ACC→GCC)	SL1344_RS07945→	virulence factor SrfB
S.Tm Alpha clone 1	STm14028	RA	NC_016810	1643641	A→G	intergenic (+59/+46)	yncL→ / ←patD	stress response membrane protein YncL/aminobutyraldehyde dehydrogenase
S.Tm Alpha clone 1	STm14028	RA	NC_016810	1677646	A→G	A25A(GCT→GCC)	SL1344_RS08120←	membrane protein
S.Tm Alpha clone 1	Novel	RA	NC_016810	1756092	G→A	D110N(GAT→AAT)	SL1344_RS08515→	DNA-binding transcriptional regulator YciT
S.Tm Alpha clone 1	STm14028	RA	NC_016810	2411272	T→C	L148L(TTA→TTG)	menC←	o-succinylbenzoate synthase
S.Tm Alpha clone 1	STm14028	RA	NC_016810	2934979	T→C	intergenic (+560/+220)	SL1344_RS14335→ / ←fljA	IS3 family transposase/phase 1 flagellin gene repressor FljA
S.Tm Alpha clone 1	STm14028	RA	NC_016810	2943604	T→C	T1152T(ACT→ACC)	iroC→	salmochelin/enterobactin export ABC transporter IroC
S.Tm Alpha clone 1	STm14028	RA	NC_016810	2943712	G→T	E1188D(GAG→GAT)	iroC→	salmochelin/enterobactin export ABC transporter IroC
S.Tm Alpha clone 2	Novel	RA	NC_016810	269042	T→A	I40N(ATC→AAC)	rnhB→	ribonuclease HII
S.Tm Alpha clone 2	STm14028	RA	NC_016810	635606	T→A	E95V(GAG→GTG)	SL1344_RS02910←	PTS system mannose/fructose/N-acetylgalactosamine-transporter subunit IIB
S.Tm Alpha clone 2	STm14028	RA	NC_016810	1638110	A→G	T55A(ACC→GCC)	SL1344_RS07945→	virulence factor SrfB
S.Tm Alpha clone 2	STm14028	RA	NC_016810	1643641	A→G	intergenic (+59/+46)	yncL→ / ←patD	stress response membrane protein YncL/aminobutyraldehyde dehydrogenase
S.Tm Alpha clone 2	STm14028	RA	NC_016810	1677646	A→G	A25A(GCT→GCC)	SL1344_RS08120←	membrane protein
S.Tm Alpha clone 2	Novel	RA	NC_016810	1756092	G→A	D110N(GAT→AAT)	SL1344_RS08515→	DNA-binding transcriptional regulator YciT
S.Tm Alpha clone 2	Novel	RA	NC_016810	2346087	C→T	A22A(GCG→GCA)	SL1344_RS11545←	cytochrome c-type biogenesis protein CcmH
S.Tm Alpha clone 2	STm14028	RA	NC_016810	2411272	T→C	L148L(TTA→TTG)	menC←	o-succinylbenzoate synthase
S.Tm Beta clone 1	STm14028	RA	NC_016810	635606	T→A	E95V(GAG→GTG)	SL1344_RS02910←	PTS system mannose/fructose/N-acetylgalactosamine-transporter subunit IIB
S.Tm Beta clone 1	STm14028	RA	NC_016810	1070375	C→T	intergenic (-234/+127)	SL1344_RS05015← / ←gtgA	hypothetical protein/type III secretion system effector protease GtgA
S.Tm Beta clone 1	Novel	RA	NC_016810	1131869	Δ1 bp	intergenic (+138/+1)	SL1344_RS05335→ / ←pipA	tRNA-Ser/type III secretion system effector protease PipA
S.Tm Beta clone 1	Novel	RA	NC_016810	1611523	T→A	intergenic (+22/-503)	yddG→ / →ompD	aromatic amino acid efflux DMT transporter YddG/porin OmpD
S.Tm Beta clone 1	Novel	RA	NC_016810	1756092	G→A	D110N(GAT→AAT)	SL1344_RS08515→	DNA-binding transcriptional regulator YciT
S.Tm Beta clone 1	STm14028	RA	NC_016810	2230940	C→T	L76L(CTG→CTA)	steD←	type III secretion system effector SteD
S.Tm Beta clone 1	Novel	RA	NC_016810	2234515	T→C	F177L(TTT→CTT)	SL1344_RS11010→	nucleoside permease
S.Tm Beta clone 1	STm14028	RA	NC_016810	2247766	A→C	R104R(CGA→CGC)	metG→	methionine--tRNA ligase
S.Tm Beta clone 1	STm14028	RA	NC_016810	2411272	T→C	L148L(TTA→TTG)	menC←	o-succinylbenzoate synthase
S.Tm Beta clone 1	STm14028	RA	NC_016810	2739383	T→G	E148D(GAA→GAC)	SL1344_RS13285←	C40 family peptidase
S.Tm Beta clone 1	Novel	RA	NC_016810	2751926	G→A	R389C(CGC→TGC)	SL1344_RS13360←	phage portal protein
S.Tm Beta clone 1	STm14028	RA	NC_016810	2752110	A→G	H327H(CAT→CAC)	SL1344_RS13360←	phage portal protein
S.Tm Beta clone 1	Novel	RA	NC_016810	2752188	G→A	P301P(CCC→CCT)	SL1344_RS13360←	phage portal protein
S.Tm Beta clone 1	Novel	RA	NC_016810	2752254	G→T	I279I(ATC→ATA)	SL1344_RS13360←	phage portal protein
S.Tm Beta clone 1	STm14028	RA	NC_016810	2757178	C→T	G131S(GGC→AGC)	SL1344_RS13390←	lysozyme
S.Tm Beta clone 1	STm14028	RA	NC_016810	4397792	G→A	intergenic (+101/-222)	SL1344_RS21340→ / →SL1344_RS21345	type III secretion system effector arginine glycosyltransferase SseK1/hypothetical protein
S.Tm Beta clone 1	STm14028	RA	NC_016810	4398551	C→A	P312P(CCG→CCT)	thiH←	2-iminoacetate synthase ThiH
S.Tm Beta clone 1	STm14028	RA	NC_016810	4402700	A→T	Y340N(TAC→AAC)	thiC←	phosphomethylpyrimidine synthase ThiC
S.Tm Beta clone 1	STm14028	RA	NC_016810	4407604	G→A	E114E(GAG→GAA)	SL1344_RS21400→	YjaG family protein
S.Tm Beta clone 1	STm14028	RA	NC_016810	4413619	T→C	T55A(ACG→GCG)	purD←	phosphoribosylamine--glycine ligase
S.Tm Beta clone 2	Novel	RA	NC_016810	234810	G→A	M22I(ATG→ATA)	SL1344_RS01005→	fimbrial protein
S.Tm Beta clone 2	STm14028	RA	NC_016810	635606	T→A	E95V(GAG→GTG)	SL1344_RS02910←	PTS system mannose/fructose/N-acetylgalactosamine-transporter subunit IIB
S.Tm Beta clone 2	STm14028	RA	NC_016810	1054847	G→T	A414E(GCA→GAA)	SL1344_RS04895←	site-specific integrase
S.Tm Beta clone 2	Novel	RA	NC_016810	1059115	A→T	W532R(TGG→AGG)	SL1344_RS04915←	RecE family exodeoxyribonuclease
S.Tm Beta clone 2	STm14028	RA	NC_016810	1061219	A→G	S32S(AGT→AGC)	SL1344_RS04925←	YdaE family protein
S.Tm Beta clone 2	STm14028	RA	NC_016810	1064445	G→A	A217T(GCG→ACG)	SL1344_RS04950→	ATP-binding protein
S.Tm Beta clone 2	STm14028	RA	NC_016810	1070375	C→T	intergenic (-234/+127)	SL1344_RS05015← / ←gtgA	hypothetical protein/type III secretion system effector protease GtgA
S.Tm Beta clone 2	Novel	RA	NC_016810	1131869	Δ1 bp	intergenic (+138/+1)	SL1344_RS05335→ / ←pipA	tRNA-Ser/type III secretion system effector protease PipA
S.Tm Beta clone 2	Novel	RA	NC_016810	1756092	G→A	D110N(GAT→AAT)	SL1344_RS08515→	DNA-binding transcriptional regulator YciT
S.Tm Beta clone 2	STm14028	RA	NC_016810	2225914	T→G	S248A(TCC→GCC)	SL1344_RS10970→	DUF4034 domain-containing protein
S.Tm Beta clone 2	STm14028	RA	NC_016810	2411272	T→C	L148L(TTA→TTG)	menC←	o-succinylbenzoate synthase
S.Tm Beta clone 2	STm14028	RA	NC_016810	2757178	C→T	G131S(GGC→AGC)	SL1344_RS13390←	lysozyme
S.Tm Beta clone 2	STm14028	RA	NC_016810	2761380	T→G	I8I(ATA→ATC)	SL1344_RS13425←	YlcG family protein
S.Tm Beta clone 2	STm14028	RA	NC_016810	2761483	A→G	C177R(TGC→CGC)	SL1344_RS13430←	recombination protein NinG
S.Tm Beta clone 2	STm14028	RA	NC_016810	2761549	C→T	A155T(GCC→ACC)	SL1344_RS13430←	recombination protein NinG
S.Tm Beta clone 2	STm14028	RA	NC_016810	2761622	G→A	F130F(TTC→TTT)	SL1344_RS13430←	recombination protein NinG
S.Tm Beta clone 2	STm14028	RA	NC_016810	2761679	T→C	A111A(GCA→GCG)	SL1344_RS13430←	recombination protein NinG

S.Tm Beta clone 2	STm14028	RA	NC_016810	2761778	T→C	K78K(AAA→AAG)	SL1344_RS13430←		recombination protein NinG
S.Tm Beta clone 2	STm14028	RA	NC_016810	2762013	T→C	intergenic (-2/+1)	SL1344_RS13430← / ←SL1344_RS27720		recombination protein NinG/hypothetical protein
S.Tm Beta clone 2	STm14028	RA	NC_016810	2762123	T→C	E33G(GAA→GGA)	SL1344_RS27720←		hypothetical protein
S.Tm Beta clone 2	STm14028	RA	NC_016810	2762157	C→T	V22I(GTA→ATA)	SL1344_RS27720←		hypothetical protein
S.Tm Beta clone 2	STm14028	RA	NC_016810	2762182	A→G	C13C(TGT→TGC)	SL1344_RS27720←		hypothetical protein
S.Tm Beta clone 2	STm14028	RA	NC_016810	2762188	G→A	H11H(CAC→CAT)	SL1344_RS27720←		hypothetical protein
S.Tm Beta clone 2	STm14028	RA	NC_016810	2762229	2 bp→CC	coding (593-594/603 nt)	SL1344_RS13440←		DUF1367 family protein
S.Tm Beta clone 2	STm14028	RA	NC_016810	2762454	T→G	A123A(GCA→GCC)	SL1344_RS13440←		DUF1367 family protein
S.Tm Beta clone 2	STm14028	RA	NC_016810	2762463	A→T	S120S(TCT→TCA)	SL1344_RS13440←		DUF1367 family protein
S.Tm Beta clone 2	STm14028	RA	NC_016810	2762472	G→C	L117L(CTC→CTG)	SL1344_RS13440←		DUF1367 family protein
S.Tm Beta clone 2	STm14028	RA	NC_016810	2762481	T→C	G114G(GGA→GGG)	SL1344_RS13440←		DUF1367 family protein
S.Tm Beta clone 2	STm14028	RA	NC_016810	2762628	G→A	P65P(CCC→CCT)	SL1344_RS13440←		DUF1367 family protein
S.Tm Beta clone 2	STm14028	RA	NC_016810	2762664	A→G	F53F(TTT→TTC)	SL1344_RS13440←		DUF1367 family protein
S.Tm Beta clone 2	Novel	RA	NC_016810	2762911	G→A	R65R(CGC→CGT)	SL1344_RS25705←		hypothetical protein
S.Tm Beta clone 2	Novel	RA	NC_016810	2763034	T→C	V24V(GTA→GTG)	SL1344_RS25705←		hypothetical protein
S.Tm Beta clone 2	Novel	RA	NC_016810	2763082	T→C	K8K(AAA→AAG)	SL1344_RS25705←		hypothetical protein
S.Tm Beta clone 2	Novel	RA	NC_016810	2763264	A→G	I64I(ATT→ATC)	SL1344_RS13450←		DinI family protein
S.Tm Beta clone 2	Novel	RA	NC_016810	2763471	C→T	intergenic (-16/+546)	SL1344_RS13450← / ←SL1344_RS13460		DinI family protein/ASCH domain-containing protein
S.Tm Beta clone 2	Novel	RA	NC_016810	2763475	C→T	intergenic (-20/+542)	SL1344_RS13450← / ←SL1344_RS13460		DinI family protein/ASCH domain-containing protein
S.Tm Beta clone 2	Novel	RA	NC_016810	2763519	G→A	intergenic (-64/+498)	SL1344_RS13450← / ←SL1344_RS13460		DinI family protein/ASCH domain-containing protein
S.Tm Beta clone 2	Novel	RA	NC_016810	2766146	T→A	M216L(ATG→TTG)	SL1344_RS13480←		replication protein P
S.Tm Beta clone 2	Novel	RA	NC_016810	2766174	T→C	S206S(TCA→TCG)	SL1344_RS13480←		replication protein P
S.Tm Beta clone 2	Novel	RA	NC_016810	2766185	C→A	A203S(GCC→TCC)	SL1344_RS13480←		replication protein P
S.Tm Beta clone 2	Novel	RA	NC_016810	2766197	G→A	R199C(CGT→TGT)	SL1344_RS13480←		replication protein P
S.Tm Beta clone 2	Novel	RA	NC_016810	2766226	A→G	V189A(GTT→GCT)	SL1344_RS13480←		replication protein P
S.Tm Beta clone 2	Novel	RA	NC_016810	2766240	C→G	E184D(GAG→GAC)	SL1344_RS13480←		replication protein P
S.Tm Beta clone 2	Novel	RA	NC_016810	2766249	A→G	I181I(ATT→ATC)	SL1344_RS13480←		replication protein P
S.Tm Beta clone 2	Novel	RA	NC_016810	2766276	T→C	K172K(AAA→AAG)	SL1344_RS13480←		replication protein P
S.Tm Beta clone 2	Novel	RA	NC_016810	2766285	G→T	L169L(CTC→TTA)	SL1344_RS13480←		replication protein P
S.Tm Beta clone 2	Novel	RA	NC_016810	2766287	G→A	L169L(CTC→TTA)	SL1344_RS13480←		replication protein P
S.Tm Beta clone 2	Novel	RA	NC_016810	2766294	T→C	E166E(GAA→GAG)	SL1344_RS13480←		replication protein P
S.Tm Beta clone 2	Novel	RA	NC_016810	2766297	2 bp→AG	coding (494-495/693 nt)	SL1344_RS13480←		replication protein P
S.Tm Beta clone 2	Novel	RA	NC_016810	2766303	C→A	R163R(CGG→CGT)	SL1344_RS13480←		replication protein P
S.Tm Beta clone 2	STm14028	RA	NC_016810	2766353	G→T	R147R(CGA→AGA)	SL1344_RS13480←		replication protein P
S.Tm Beta clone 2	STm14028	RA	NC_016810	2766357	T→G	P145P(CCA→CCC)	SL1344_RS13480←		replication protein P
S.Tm Beta clone 2	Novel	RA	NC_016810	2767678	2 bp→CA	coding (15-16/906 nt)	SL1344_RS13485←		replication protein
S.Tm Beta clone 2	Novel	RA	NC_016810	2767744	2 bp→AC	intergenic (-51/+40)	SL1344_RS13485← / ←SL1344_RS13490		replication protein/CII family transcriptional regulator
S.Tm Beta clone 2	Novel	RA	NC_016810	2767747	3 bp→CCT	intergenic (-54/+36)	SL1344_RS13485← / ←SL1344_RS13490		replication protein/CII family transcriptional regulator
S.Tm Beta clone 2	Novel	RA	NC_016810	2767771	A→G	intergenic (-78/+14)	SL1344_RS13485← / ←SL1344_RS13490		replication protein/CII family transcriptional regulator
S.Tm Beta clone 2	Novel	RA	NC_016810	2767778	G→A	intergenic (-85/+7)	SL1344_RS13485← / ←SL1344_RS13490		replication protein/CII family transcriptional regulator
S.Tm Beta clone 2	Novel	RA	NC_016810	2767887	T→C	E91E(GAA→GAG)	SL1344_RS13490←		CII family transcriptional regulator
S.Tm Beta clone 2	Novel	RA	NC_016810	2767908	C→T	G84G(GGG→GGA)	SL1344_RS13490←		CII family transcriptional regulator
S.Tm Beta clone 2	Novel	RA	NC_016810	2767947	C→T	G71G(GGG→GGA)	SL1344_RS13490←		CII family transcriptional regulator
S.Tm Beta clone 2	Novel	RA	NC_016810	2767962	C→T	R66R(AGG→AGA)	SL1344_RS13490←		CII family transcriptional regulator
S.Tm Beta clone 2	Novel	RA	NC_016810	2768004	T→A	S52S(TCA→TCT)	SL1344_RS13490←		CII family transcriptional regulator
S.Tm Beta clone 2	Novel	RA	NC_016810	2768043	A→G	S39S(AGT→AGC)	SL1344_RS13490←		CII family transcriptional regulator
S.Tm Beta clone 2	Novel	RA	NC_016810	2768052	C→T	E36E(GAG→GAA)	SL1344_RS13490←		CII family transcriptional regulator
S.Tm Beta clone 2	Novel	RA	NC_016810	2770674	G→A	pseudogene (39/156 nt)	SL1344_RS27725→		hypothetical protein
S.Tm Beta clone 2	Novel	RA	NC_016810	2770718	T→C	pseudogene (83/156 nt)	SL1344_RS27725→		hypothetical protein
S.Tm Beta clone 2	Novel	RA	NC_016810	2770722	T→C	pseudogene (87/156 nt)	SL1344_RS27725→		hypothetical protein
S.Tm Beta clone 2	STm14028	RA	NC_016810	4397792	G→A	intergenic (+101/-222)	SL1344_RS21340→ / →SL1344_RS21345		type III secretion system effector arginine glycosyltransferase SseK1/hypothetical protein
S.Tm Beta clone 2	STm14028	RA	NC_016810	4398551	C→A	P312P(CCG→CCT)	thiH←		2-iminoacetate synthase ThiH
S.Tm Beta clone 2	STm14028	RA	NC_016810	4402700	A→T	Y340N(TAC→AAC)	thiC←		phosphomethylpyrimidine synthase ThiC
S.Tm Beta clone 2	STm14028	RA	NC_016810	4407604	G→A	E114E(GAG→GAA)	SL1344_RS21400→		YjaG family protein
S.Tm Beta clone 2	STm14028	RA	NC_016810	4413619	T→C	T55A(ACG→GCG)	purD←		phosphoribosylamine--glycine ligase
S.Tm Gamma clone 1	STm14028	RA	NC_016810	635606	T→A	E95V(GAG→GTG)	SL1344_RS02910←		PTS system mannose/fructose/N-acetylgalactosamine-transporter subunit IIB

S.Tm Gamma clone 1	Novel	RA	NC_016810	1092165	C→T	A116V(GCA→GTA)	SL1344_RS27640→	DUF1983 domain-containing protein
S.Tm Gamma clone 1	STm14028	RA	NC_016810	1100366	A→G	intergenic (-330/-97)	SL1344_RS05185← / →pepN	DinI-like family protein/aminopeptidase N
S.Tm Gamma clone 1	STm14028	RA	NC_016810	1110819	A→G	I191V(ATC→GTC)	pqiA→	membrane integrity-associated transporter subunit PqiA
S.Tm Gamma clone 1	STm14028	RA	NC_016810	1113716	G→T	intergenic (+9/-247)	pqiC→ / →rmf	membrane integrity-associated transporter subunit PqiC/ribosome modulation factor
S.Tm Gamma clone 1	Novel	RA	NC_016810	1756092	G→A	D110N(GAT→AAT)	SL1344_RS08515→	DNA-binding transcriptional regulator YciT
S.Tm Gamma clone 1	STm14028	RA	NC_016810	2411272	T→C	L148L(TTA→TTG)	menC←	o-succinylbenzoate synthase
S.Tm Gamma clone 1	Novel	RA	NC_016810	2733854	G→T	T311N(ACT→AAT)	SL1344_RS13265←	prophage tail fiber N-terminal domain-containing protein
S.Tm Gamma clone 1	STm14028	RA	NC_016810	2739383	T→G	E148D(GAA→GAC)	SL1344_RS13285←	C40 family peptidase
S.Tm Gamma clone 1	STm14028	RA	NC_016810	4686205	G→T	P47H(CCT→CAT)	SL1344_RS26225←	hypothetical protein
S.Tm Gamma clone 1	STm14028	RA	NC_016810	4686380	+T	intergenic (-36/-86)	SL1344_RS26225← / →reiD	hypothetical protein/myo-inositol utilization transcriptional regulator ReiD
S.Tm Gamma clone 1	STm14028	RA	NC_016810	4693227	T→C	S570G(AGT→GGT)	iolC←	5-dehydro-2-deoxygluconokinase
S.Tm Gamma clone 1	STm14028	RA	NC_016810	4694618	A→C	V106G(GTC→GGC)	iolC←	5-dehydro-2-deoxygluconokinase
S.Tm Gamma clone 1	STm14028	RA	NC_016810	4695137	T→C	intergenic (-203/-214)	iolC← / →iolD	5-dehydro-2-deoxygluconokinase/3D-(3,5/4)-trihydroxycyclohexane-1,2-dione acylhydrolase (decyclizing)
S.Tm Gamma clone 2	STm14028	RA	NC_016810	635606	T→A	E95V(GAG→GTG)	SL1344_RS02910←	PTS system mannose/fructose/N-acetylgalactosamine-transporter subunit IIB
S.Tm Gamma clone 2	Novel	RA	NC_016810	1756092	G→A	D110N(GAT→AAT)	SL1344_RS08515→	DNA-binding transcriptional regulator YciT
S.Tm Gamma clone 2	STm14028	RA	NC_016810	2225914	T→G	S248A(TCC→GCC)	SL1344_RS10970→	DUF4034 domain-containing protein
S.Tm Gamma clone 2	STm14028	RA	NC_016810	2411272	T→C	L148L(TTA→TTG)	menC←	o-succinylbenzoate synthase
S.Tm Gamma clone 2	Novel	JC	NC_016810	2728635	(GGGCAA)8→10	intergenic (+449/-24)	gogB→ / →SL1344_RS25680	type III secretion effector GogB/PagK family vesicle-borne virulence factor
S.Tm Gamma clone 2	Novel	RA	NC_016810	4274092	C→T	M35I(ATG→ATA)	SL1344_RS20770←	AzlC family ABC transporter permease
S.Tm Gamma clone 2	STm14028	RA	NC_016810	4686205	G→T	P47H(CCT→CAT)	SL1344_RS26225←	hypothetical protein
S.Tm Gamma clone 2	STm14028	RA	NC_016810	4686380	+T	intergenic (-36/-86)	SL1344_RS26225← / →reiD	hypothetical protein/myo-inositol utilization transcriptional regulator ReiD
S.Tm Gamma clone 2	STm14028	RA	NC_016810	4693227	T→C	S570G(AGT→GGT)	iolC←	5-dehydro-2-deoxygluconokinase
S.Tm Gamma clone 2	STm14028	RA	NC_016810	4694618	A→C	V106G(GTC→GGC)	iolC←	5-dehydro-2-deoxygluconokinase
S.Tm Gamma clone 2	STm14028	RA	NC_016810	4695137	T→C	intergenic (-203/-214)	iolC← / →iolD	5-dehydro-2-deoxygluconokinase/3D-(3,5/4)-trihydroxycyclohexane-1,2-dione acylhydrolase (decyclizing)
S.Tm Delta clone 1	STm14028	RA	NC_016810	635606	T→A	E95V(GAG→GTG)	SL1344_RS02910←	PTS system mannose/fructose/N-acetylgalactosamine-transporter subunit IIB
S.Tm Delta clone 1	Novel	RA	NC_016810	1746596	C→A	intergenic (-53/+414)	SL1344_RS08470← / ←steC	EAL domain-containing protein/SPI-2 type III secretion system effector kinase SteC
S.Tm Delta clone 1	STm14028	RA	NC_016810	1748808	A→G	G79G(GGA→GGG)	SL1344_RS08485→	hypothetical protein
S.Tm Delta clone 1	Novel	RA	NC_016810	1756092	G→A	D110N(GAT→AAT)	SL1344_RS08515→	DNA-binding transcriptional regulator YciT
S.Tm Delta clone 1	STm14028	RA	NC_016810	2411272	T→C	L148L(TTA→TTG)	menC←	o-succinylbenzoate synthase
S.Tm Delta clone 2	Novel	RA	NC_016810	83119	T→A	G334G(GGA→GGT)	caiC←	crotonobetaine/carnitine-CoA ligase
S.Tm Delta clone 2	STm14028	RA	NC_016810	635606	T→A	E95V(GAG→GTG)	SL1344_RS02910←	PTS system mannose/fructose/N-acetylgalactosamine-transporter subunit IIB
S.Tm Delta clone 2	Novel	RA	NC_016810	1746596	C→A	intergenic (-53/+414)	SL1344_RS08470← / ←steC	EAL domain-containing protein/SPI-2 type III secretion system effector kinase SteC
S.Tm Delta clone 2	STm14028	RA	NC_016810	1748808	A→G	G79G(GGA→GGG)	SL1344_RS08485→	hypothetical protein
S.Tm Delta clone 2	Novel	RA	NC_016810	1756092	G→A	D110N(GAT→AAT)	SL1344_RS08515→	DNA-binding transcriptional regulator YciT
S.Tm Delta clone 2	STm14028	RA	NC_016810	2411272	T→C	L148L(TTA→TTG)	menC←	o-succinylbenzoate synthase
S.Tm Delta clone 2	Novel	RA	NC_016810	2770504	G→T	intergenic (-120/-132)	SL1344_RS13510← / →SL1344_RS27725	hypothetical protein/hypothetical protein
S.Tm Epsilon clone 1	STm14028	RA	NC_016810	635606	T→A	E95V(GAG→GTG)	SL1344_RS02910←	PTS system mannose/fructose/N-acetylgalactosamine-transporter subunit IIB
S.Tm Epsilon clone 1	STm14028	RA	NC_016810	876446	T→G	E388A(GAG→GCG)	clsB←	cardiolipin synthase ClsB
S.Tm Epsilon clone 1	STm14028	RA	NC_016810	1677646	A→G	A25A(GCT→GCC)	SL1344_RS08120←	membrane protein
S.Tm Epsilon clone 1	Novel	RA	NC_016810	1756092	G→A	D110N(GAT→AAT)	SL1344_RS08515→	DNA-binding transcriptional regulator YciT
S.Tm Epsilon clone 1	STm14028	RA	NC_016810	2411272	T→C	L148L(TTA→TTG)	menC←	o-succinylbenzoate synthase
S.Tm Epsilon clone 2	STm14028	RA	NC_016810	635606	T→A	E95V(GAG→GTG)	SL1344_RS02910←	PTS system mannose/fructose/N-acetylgalactosamine-transporter subunit IIB
S.Tm Epsilon clone 2	Novel	RA	NC_016810	732867	A→T	L276Q(CTG→CAG)	SL1344_RS03380←	PhoH family protein
S.Tm Epsilon clone 2	Novel	RA	NC_016810	1473226	C→T	H109Y(CAT→TAT)	sodC2→	superoxide dismutase [Cu-Zn] SodC2
S.Tm Epsilon clone 2	STm14028	RA	NC_016810	1677646	A→G	A25A(GCT→GCC)	SL1344_RS08120←	membrane protein
S.Tm Epsilon clone 2	Novel	RA	NC_016810	1756092	G→A	D110N(GAT→AAT)	SL1344_RS08515→	DNA-binding transcriptional regulator YciT
S.Tm Epsilon clone 2	STm14028	RA	NC_016810	2411272	T→C	L148L(TTA→TTG)	menC←	o-succinylbenzoate synthase
S.Tm Epsilon clone 2	STm14028	RA	NC_016810	3964111	C→T	L12L(CTG→TTG)	SL1344_RS19305→	AsmA family protein
S.Tm Epsilon clone 2	STm14028	RA	NC_016810	3973364	C→T	R106R(CGC→CGT)	SL1344_RS19340→	virulence RhuM family protein
S.Tm Epsilon clone 2	STm14028	RA	NC_016810	3974959	A→G	intergenic (-590/-424)	SL1344_RS26075← / →SL1344_RS19345	transposase/helix-turn-helix transcriptional regulator
S.Tm Zeta clone 1	STm14028	RA	NC_016810	635606	T→A	E95V(GAG→GTG)	SL1344_RS02910←	PTS system mannose/fructose/N-acetylgalactosamine-transporter subunit IIB
S.Tm Zeta clone 1	Novel	RA	NC_016810	1756092	G→A	D110N(GAT→AAT)	SL1344_RS08515→	DNA-binding transcriptional regulator YciT
S.Tm Zeta clone 1	STm14028	RA	NC_016810	2411272	T→C	L148L(TTA→TTG)	menC←	o-succinylbenzoate synthase
S.Tm Zeta clone 1	STm14028	RA	NC_017720	64311	A→G	L146L(CTA→CTG)	spvB→	SPI-2 type III secretion system effector NAD(+)--protein-arginine ADP-ribosyltransferase SpvB
S.Tm Zeta clone 1	Novel	JC	NC_017720	69582	(TCATGGCCG)2→1	coding (44-52/603 nt)	SL1344_RS27810←	LysM peptidoglycan-binding domain-containing protein
S.Tm Zeta clone 2	STm14028	RA	NC_016810	635606	T→A	E95V(GAG→GTG)	SL1344_RS02910←	PTS system mannose/fructose/N-acetylgalactosamine-transporter subunit IIB

S.Tm Zeta clone 2	Novel	RA	NC_016810	1756092	G→A	D110N(GAT→AAT)	SL1344_RS08515→	DNA-binding transcriptional regulator YciT
S.Tm Zeta clone 2	STm14028	RA	NC_016810	2411272	T→C	L148L(TTA→TTG)	menC←	o-succinylbenzoate synthase
S.Tm Zeta clone 2	STm14028	RA	NC_017720	64311	A→G	L146L(CTA→CTG)	spvB→	SPI-2 type III secretion system effector NAD(+)--protein-arginine ADP-ribosyltransferase SpvB
S.Tm Zeta clone 2	Novel	JC	NC_017720	69582	(TCATGGCCG)2→1	coding (44-52/603 nt)	SL1344_RS27810←	LysM peptidoglycan-binding domain-containing protein